University of South-Eastern Norway

www.usn.no

FMH606 Master's Thesis 2022

Process Technology

Laminar Burning Velocity in Hydrogen-Oxygen-Nitrogen Mixtures

YONE KYIN THANG

Faculty of Technology, Natural Sciences and Maritime Sciences
Campus Porsgrunn

University of South-Eastern Norway

www.usn.no

Course: FMH606 Master's Thesis, 2022

Title: Laminar burning velocity in hydrogen-oxygen-nitrogen mixtures

Number of pages: 69

Keywords: Laminar burning velocity, hydrogen-oxygen-nitrogen mixture, gas explosion, Cantera

Student: Yone Kyin Thang

Supervisor: Prof. Dag Bjerketvedt, Post-Doc. Mathias Henriksen, Prof. Knut Vaagsaether

External partner: **MoZEES and Corvus**

University of South-Eastern Norway

www.usn.no

Summary:

As today's world is demanding a greener environment where greenhouse gas emission and global warming are much reduced, hydrogen has become the most promising element among others from periodic table. As today's world is demanding a greener environment where greenhouse gas emission and global warming are much reduced, hydrogen has become the most promising element among others from the periodic table. Combustion of hydrogen has been observed as a renewable and efficient green method to replace the burning of hydrocarbon fuels with higher efficiency in the combustion systems. Even though hydrogen can be efficient in some ways, there are different factors that can be hazardous to the environment as well as to human beings. Due to the safety reasons for hydrogen utilization in the combustion systems, the required studies have been done to investigate the behaviors of hydrogen while mitigating the problems for safety purposes. In order to replace energy sources from fossil fuels, a required predictive and reliable modeling such as the laminar premixed burning velocity of the mixture is mainly used. In the method, the chemical reactions during the combustion process are based on and studied to proceed with the evaluation of the laminar burning velocity of the hydrogen-oxygen- nitrogen mixture. For numerical computations of chemical reactions and laminar burning flame speed, the chemical kinetics model and the tool Cantera are used. In the present study, the laminar burning velocity of the hydrogen-oxygen-nitrogen mixture is evaluated to find how hydrogen explosion in a confined space can be mitigated by varying the oxygen concentration. The concept that reducing oxygen concentration in the cloud can decrease the heat release and laminar burning velocity of the premixed gas is proposed. The study aims to find the burning velocity in hydrogen-oxygen-nitrogen mixtures by performing experiments in a 20-liter explosion vessel. The evaluation of laminar burning velocity is done on different concentrations of the mixture and different ignition energy. The literature study is first done, and the experiments are performed to investigate the laminar flame speed, Markstein length, stretch rate, and laminar burning velocity. Besides, the simulation tool Cantera is used to calculate the laminar burning velocity of the mixture and to validate the mechanisms and methods used in this study.

Preface

The observation in evaluating the laminar burning velocity in hydrogen-oxygen-nitrogen mixtures with experiments performed in a 20-liter explosion vessel is presented in this report. Firstly, I would like to express my gratitude to the program coordinator for granting us the thesis topic I have prioritized. I am also grateful to work under the invaluable guidance and kind assistance of supervisor Prof. Dag Bjerketvedt and co-supervisor Post-Doc. Mathias Henriksen. Their help and support, particularly during the experiments and writing-up period, are much appreciated. Finally, my thanks go to my family back from Myanmar, my uncle's family from Norway, my mentors, my teachers, and all my friends who have supported me motivationally, emotionally, financially, and technically during my study in Norway.

Porsgrunn, May 18, 2022

Yone Kyin Thang

Contents

Nomenclature

Symbol	Description	Units
A	Area	m^2
L	Length	m
R^2	Coefficient of Determination	-
S	Flame speed	$m.s^{-1}$
S_b	Premixed laminar flame propagation	$m.s^{-1}$
S_u^0	Laminar burning velocity	$m.s^{-1}$
S_b^0	Laminar flame speed	$m.s^{-1}$
T	Temperature	K
Y	Mass Fraction	-
L_b	Markstein Length	m
h	Enthalpy	$J.g^{-1}$
p	Pressure	Pa, bar
r_f	Flame radius	m
t	Time	s
u	Velocity	$m.s^{-1}$
κ	Stretch Rate	s^{-1}
ρ_u	Density of unburnt gas mixture	$kg\ m^{-3}$
ρ_b	Density of burnt gas mixture	$kg\ m^{-3}$
ϕ	Fuel-Air Equivalence Ratio	-
λ	Air-Fuel Equivalence Ratio	-

List of Tables

List of Figures

1 Introduction

Since the industrial revolution, energy, and power demands have been increasing with the development in technology and production methods. In energy production, energy from the combustion of high energy density carbon-based fuels (fossil-based sources) became the main source. The majority of the power supply to the energy grid comes from fossil-based fuels. However, unfortunately, the dependence on fossil-based fuels leads to environmental problems such as pollution, an increase in greenhouse gases, and global warming. Despite the high availability of carbon-based fuels, there are also alternatives to produce energy and power with higher efficiency maintaining a high standard of living while securing natural resources. Hence, the necessary technology is being developed to replace carbon-based fuels with renewable energy sources and alternative fuels such as hydrogen to meet the energy demands while reducing climate change, pollution, and global warming.

In this study, the properties and relevant study on alternative fuel as hydrogen will be described concerning safety purposes. Hydrogen has become the most promising gas for the combustion process to generate power and for transportation applications for its high efficiency. It can be produced from the excess energy from renewable energy sources such as solar and wind energy. Like the products, water and oxygen are only released from the combustion of hydrogen-air mixtures. While the combustion process gives efficient energy and power generation, the explosion intensity of hydrogen has also become an issue to consider for the safety aspects. To study the hydrogen explosion and its behaviors, the concentrations of fuel (hydrogen) and oxidant are needed to vary and tested under different equivalence ratios.

The investigation of combustion characteristics of gas mixtures can be done with predictable models for chemical reactions and chemical kinetics. In order to measure the intensity of the explosion, the laminar premixed burning velocity of hydrogen is also important to evaluate. Evaluation of laminar burning velocity will be emphasized in the present study to examine the explosion characteristics. Experiments are mainly conducted to evaluate laminar flame speed with different gas compositions. From the experiments with developed image processing python codes developed and used by Mathias [2], the flame speeds are evaluated, and laminar burning velocities are calculated with the linear stretch extrapolation method. On the other hand, the tool Cantera integrated with python software is used to perform the numerical calculations. From experimental results and numerical calculations, the laminar flame speed, stretch rate, Markstein length, and laminar burning velocity are investigated and presented in later chapters.

Therefore, an evaluation of laminar burning velocity is needed to examine the mitigation of hydrogen explosion in confined space with different oxygen concentrations in the cloud of the premixed gas.

1.1 Aim and Objectives

The main aim is to find the laminar burning velocity in hydrogen-oxygen-nitrogen mixtures by performing experiments in a 20-liter explosion vessel.

The Objectives are to:

- Perform a literature study on laminar burning velocity in hydrogen-oxygen-nitrogen mixtures.
- Use Cantera to simulate laminar burning velocity in hydrogen-oxygen-nitrogen
- Do experiments with a 20-liter explosion vessel with hydrogen-oxygen-nitrogen mixtures.
- Find laminar flame speeds in hydrogen-oxygen-nitrogen mixtures from high-speed videos.
- Compare predicted and measured laminar burning velocities.

1.2 Approach

In the present work, experiments in a 20-liter explosion vessel with different hydrogen-oxygen-nitrogen mixtures were performed. From the recorded videos of each experiment, flame speeds were evaluated with the help of the linear stretch (LS) model and python programming codes. Then, numerical calculations on laminar burning velocity were done with the tool Cantera integrated with python software to make a comparative study.

1.3 Outline of thesis

In chapter 1, the general introduction with a few backgrounds of hydrogen is presented along with the aim and objectives. In addition, the approach and outline of the thesis are also presented. Chapter 2 reviews previous works on the determination of the laminar burning velocity of different gas mixtures, the theory and method used, and the fundamentals of combustion processes. The experimental setup and procedure used for all experiments are described in Chapter 3. Moreover, Chapter 4 elaborates on the method and tools used in work for evaluating laminar burning velocity. The results obtained from experiments and numerical calculations done with Cantera were summarized in Chapter 5. Finally, Chapter 6 presents the main conclusion and suggestions for refinements through future scope, followed by the references section in Chapter 7 and appendices in Chapter 8.

2 Literature Review and Theory

In this chapter, previous useful works on finding the laminar burning velocity of different gas mixtures where relevant theory and approach can be applied are reviewed. Relevant combustion theory related to the chemical kinetic of hydrogen-oxygen and nitrogen is also presented as a review in the following sections.

2.1 Laminar burning velocities of diluted hydrogen-oxygen-nitrogen mixtures

This section summarizes the analysis and measurements of laminar adiabatic burning velocities of flames propagating in hydrogen-oxygen-nitrogen mixtures at atmospheric pressure.

2.1.1 Background of study

The burning velocity as an important characteristic in combustion processes was analyzed to study the properties of the given hydrogen-oxygen-nitrogen mixtures. It is also presented that the burning velocity is one of the key parameters which also governs the flames stabilization.

In order to validate the reaction mechanisms, the experimental measurements of laminar burning velocities were performed. As the numerical approach, the heat flux method was introduced to obtain accurate measurements of the adiabatic burning velocity and the propagation of adiabatic laminar premixed flames in hydrogen-oxygen-nitrogen mixtures was studied experimentally. In the experiment, the oxygen content in the oxidizer, $O_2/(O_2+N_2)$, was varied between 0.07 and 0.1077. The fuel equivalence ratio (ϕ) was varied between 0.7 and 3.1. Finally, the results were compared with other experimental data and numerical results using a detailed chemical kinetics mechanism.

2.1.2 Method and results

The heat flux burner was used to perform the experiments. The detailed descriptions of the heat flux method and experimental setup can be found in the articles [3], [4].

One of the experimental results of the laminar burning velocity can be found in Figure (2.1). In the figure, it can be found that the results are compared with the experimental data of Egolfopoulos and law [1] and numerical simulations. The experiments were performed with a gas flow temperature of 298 K and ambient pressure. In Figure (2.1), the results with constant $\phi = 1.058$ and varying oxygen content in the oxidizer, $O_2/(O_2+N_2)$ are presented. In this brief review, the most relevant parts of the paper to the present work are only included. Moreover, the results at some points from the experiments on varying oxygen content in the oxidizer, $O_2/(O_2+N_2)$ will be compared with the experimental results obtained in the present work. Therefore, it is recommended to study the detailed approach, theory, and method in the referred article [5].

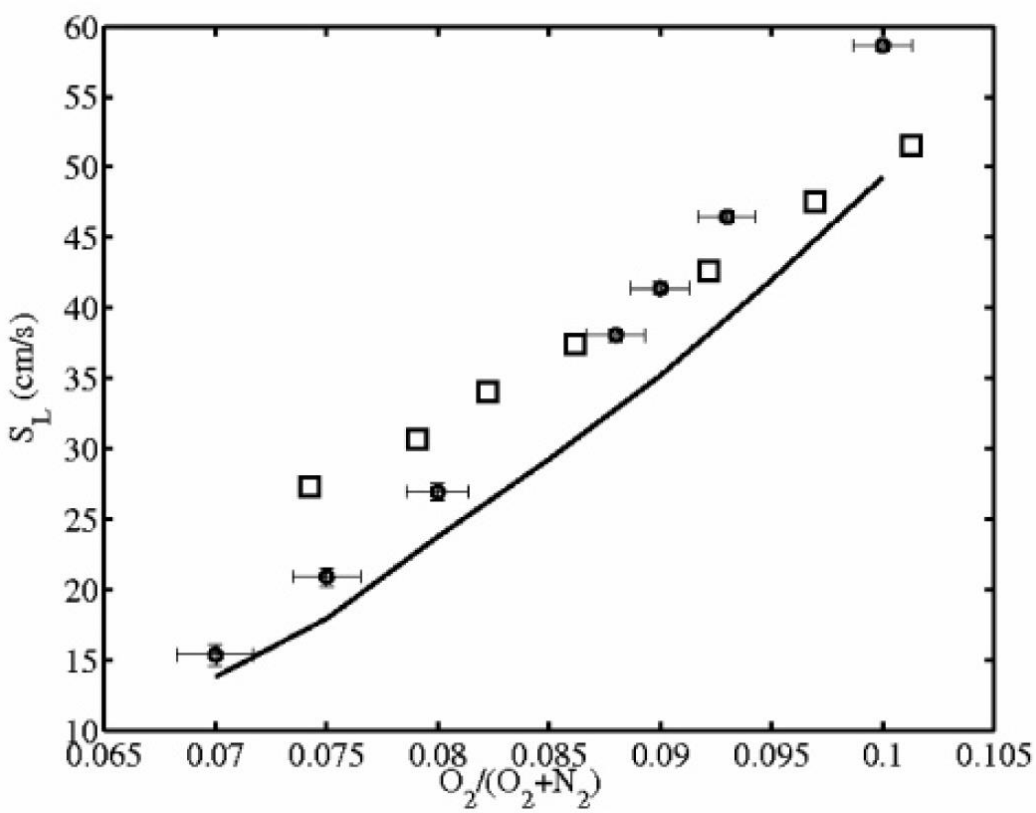

Figure 2.1. Laminar burning velocities of H_2-O_2-N_2 mixtures at an equivalence ratio of 1.058 with different oxygen fractions in the oxidizer stream. The measurements and modeling were performed with a gas flow temperature of 298 K and ambient pressure. Circles, heat flux measurements; squares, measurements by Egolfopoulos and Law[1]; and line, calculations.

2.2 Laminar burning velocity of the dimethyl carbonate-air mixture formed by the Li-Ion electrode solvent

In this section, the experimental approaches and calculation methods used in the paper were reviewed and discussed. The original purpose of the paper is to experimentally determine the laminar burning velocity and the Markstein length for dimethyl carbonate and propane in a 20-liter explosion sphere [6].

2.2.1 Description of experimental setup

As described earlier, a 20-liter explosion sphere is used to perform experiments. The sphere is a closed volume type with three inlet ports where fuel and oxidizer can be added. To keep the sphere at the ambient temperature, a heating jacket is used where the jacket is heated with a separate heating system. A heating plate under the sphere is also used to evaporate liquids. During the experiment, the ambient pressure and explosion pressure are measured with pressure transducers. A motorized stirrer and ignition system are also equipped in the sphere. For image capturing from the explosion inside the sphere, a high-speed video camera is

utilized. All the data outputs such as explosion pressure and images are recorded with the oscilloscope and specified computer software for the camera, respectively.

2.2.2 Theory and methods

After performing the experiments with a 20-liter explosion sphere, the images recorded are further processed and analyzed with the code generated in Python. From the image processing, the radii at different time are produced and used in the flame speed formula to calculate the flame speed with respect to the burnt state. The general Equation to calculate the flame speed by considering the raw data from flame propagation is described as follows;

$$S_b(t) = \frac{dr_f(t)}{dt} = \frac{r_{f,2} - r_{f,1}}{t_2 - t_1} \quad (1)$$

where r_f is flame radius and t is time.

After calculating the flame speed through the temporal evolution of the radius, the relevant laminar flame speed and Markstein length are calculated using the following stretch rate equation and stretch extrapolation models shown in the Table (2.1).

$$\kappa = \frac{1}{A_f} \cdot \frac{dA_f}{dt} = \frac{2S_b}{r_f} \quad (2)$$

where κ is the stretch rate and A is the area.

Table 2.1. Stretch extrapolation models [6]

Model name/description	Expression	References
Linear stretch (LS) model	$S_b = S_b^0 - L_b\kappa$	[7]
Linear curvature (LC) model	$S_b = S_b^0\left(1 - \frac{2L_b}{r_f}\right)$	[8], [9]
Non-linear model with 3 fitting parameters (N3P)	$S_b = S_b^0\left(1 - \frac{2L_b}{r_f} + \frac{c}{r_f^2}\right)$	[10]
Non-linear (NQ) model in expansion form	$S_b^0 + c = r_f + 2L_b \ln(r_f) - \frac{4L_b^2}{r_f} - \frac{8L}{3r}$	[11]
Quasi-steady (NE) non-linear model	$\left(\frac{S_b}{S_b^0}\right)^2 \cdot ln\left(\frac{S_b}{S_b^0}\right) = -\frac{4L_b\kappa}{S_b^0}$	[12], [13]

Laminar flame speed is calculated using the linear stretch (LS) model from Table (2.1) by extrapolating the stretch rate to zero and the laminar burning velocity (LBV) is calculated using Equation (3) with the assumption of equilibrium between burnt and unburnt states.

$$S_u^0\rho_u = S_b^0\rho_b \quad (3)$$

Where S_u^0 is the laminar burning velocity (LBV) with respect to the unburnt state, ρ_u, and ρ_b are the densities of unburnt and burnt gas mixture and S_b^0 is the laminar flame speed.

Along with the experimental analysis, calculation of the equilibrium states and the laminar burning velocity (LBV) for constant pressure combustion is done with the simulation tool Cantera (version 2.3.0) [14]. FreeFlame, the composite domain for a one-dimensional freely propagating planar flame, is used to calculate the LBV. The comparison between experimental results and the results from Cantera is made with plots.

Since the focus of this review is limited to the study of laminar burning velocity (LBV) and Markstein length, the main results from the study will not be discussed. For a comprehensive review, the Ph.D. dissertation "A study of premixed combustion of gas vented from failed Li-ion batteries" by Mathias Henriksen is recommended.

2.3 A comprehensive review of measurements and data analysis of laminar burning velocities for various fuel mixtures

This part reviews numerical analysis of laminar premixed flames and laminar burning velocity of hydrogen and air mixtures.

2.3.1 Background of study

In this literature, the laminar burning velocities of different fuel and air mixtures are reviewed with the analysis of the numerical and experimental findings using different methods. It was intended to develop the accuracy in measurement and prediction of laminar burning velocity for the understanding the variation of LBV is crucial in practical applications such as rocket engines, industrial furnaces, and gas turbine combustors as they are operated under higher temperatures and pressures than ambient conditions. In the article, the existing laminar burning velocity data of different fuel mixtures such as hydrogen and air mixtures are reviewed to observe the effect of thermodynamics parameters such as equivalence ratio, temperature, and pressure of the given mixture on the variation of laminar burning velocity (LBV). The spherical flame method [15]is used in the literature with a spark ignition system at the center, and the flame propagation speed is evaluated from flame radius with time [16], [17].

2.3.2 Spherical flame method

At a given initial temperature and pressure conditions, a premixed fuel and air mixture with a known equivalence ratio is added in a closed spherical chamber. With the ignition source at the vessel's center, the fuel and air mixture is ignited to produce a spherical flame propagation into a quiescent combustible mixture. According to the literature, it is found that unsteady flame propagation, flame curvature variation, diffusional effects, and non-uniform flow field effect flame properties of spherical expanding flame. These effects are also concluded as flame stretch effects and impact the flame propagation speed of the mixture [17]. Therefore, it is important to examine the stretch effects to derive unstretched laminar burning velocity (LBV)

from the raw measurements. Two different methods as constant pressure method and the constant volume method, are introduced as the most useful spherical flame methods in estimating LBV. Nevertheless, in the current study, the constant volume method with optical access will be used to record and measure the flame propagation.

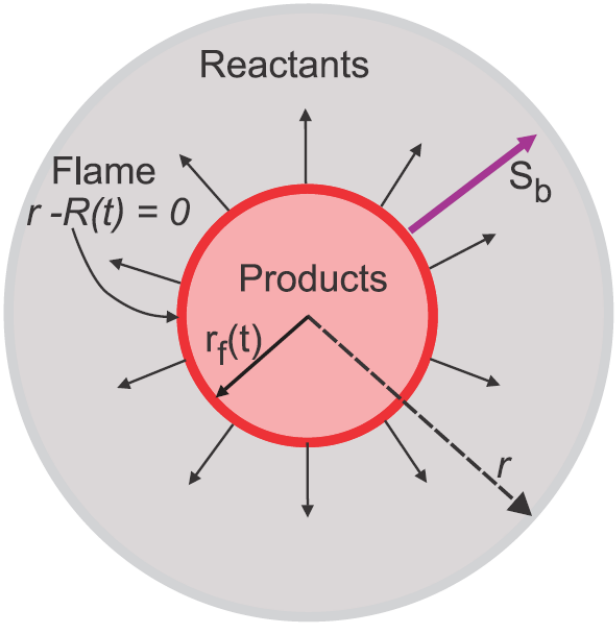

Figure 2.2. Outwardly spherical propagating flame into the quiescent premixed combustible mixture. S_b refers to premixed laminar flame propagation, and $r_f(t)$ refers to the instantaneous flame front radius, and r is the vessel radius. [18]

2.3.3 Numerical analysis of laminar premixed flames

Along with relevant reaction mechanisms, one-dimensional laminar premixed flame equations are solved to determine various aspects of laminar burning velocity. Using numerical tools gives an important understanding of the aspects, including the importance of radiation, pressure, temperature, equivalence ratio, sensitivity, and characteristic of species in the combustion process in evaluating laminar burning velocity. A calculation method for one-dimensional unsteady laminar flame propagation based on a two-dimensional boundary layer model proposed by Spalding can be found in the referred articles [19], [20] where the methodology is applied for calculating LBV for hydrogen and oxygen flames. Unsteady conservation equations modeled by Warnatz for one-dimensional laminar premixed flames for hydrogen, oxygen, and air mixtures is also provided in the referred articles [21], [22]. The numerical codes used in this literature are also presented for computing laminar burning velocities. As the summary of various numerical codes, a comparison of various numerical tools and codes for simulations is made in the following Table (2.2).

Table 2.2. A brief summary of various numerical codes [18]

Tool/Code	Capabilities	Method	Discretization scheme	References
PREMIX/OPPDIFF	FPF, CPF	FDM	2nd Order Upwind	[23], [24]
CANTERA	FPF, CPF	FDM	2nd Order Upwind	[14]
FLAMEMASTER	FPF, CPF			[25]
COSILAB/RUN1DL	FPF, CPF, OPF	FDM	2nd Order Upwind	[26]
CHEM1D	FPF, CPF, OPF	FVM	2nd Order Upwind	[27]
ASURF1D	FPF, CPF, OPF	FVM	2nd Order Upwind	[28]
OPENSMOKE++	FPF, CPF	FVM	2nd Order Upwind	[29]
AGNISOFT	FPF, CPF	FVM	2nd Order Upwind	[30]

Abbreviations

FPF – Freely propagating flame

CPF – Stagnation flame/Counterflow premixed flame

OPF – Outwardly propagating spherical flames

FDM – Finite difference method

FVM – Finite volume method

The comparative study is done to observe the difference and accuracy of each tool. Among them, the application of CANTERA is only focused on as it will be used in this study. Laminar flame speed and laminar burning velocity are generated with respect to initial conditions of temperature and pressure, equivalence ratio and gas composition of the mixture, and the optimized reaction mechanism (GRI-Mech 3.0). In this way, the approach and procedure of evaluating laminar burning velocity with CANTERA are referred in this literature.

2.3.4 Laminar burning velocity of hydrogen and air mixtures

Laminar burning velocity measurements with respect to equivalence ratio at standard conditions: atmospheric pressure and initial temperature of the mixtures are presented with previous works to study the mixture dependence of hydrogen and air flames.

The spherical flame with the linear model suggested by Markstein [31] is used to calculate the laminar burning velocity. According to the previous studies, it is summarized that the most

important issue affecting the burning velocity derived with the spherical flame method is a stretch correction which is applied in calculating laminar flame speed [18]. It is also found that the results obtained from calculating the burning velocity of hydrogen flames could be unreliable if the proper procedures of stretch extrapolation are not done [18]. In addition, the temperature and pressure dependence of hydrogen and air flames are discussed. Since the analysis of this literature is mainly done on the variation of LBV calculation method versus variations in equivalence ratio, experimental and numerical results will be taken to make a comparative literature study. Therefore, the rest of the detailed analytical methods or approaches done in this literature can be found in the full paper version of the article [32].

2.4 Fundamentals of combustion processes

2.4.1 Premixed flames

Flames have complex systems with different chemical and physical properties. For these reasons, there are still no satisfactory methods to predict the properties of flames. In studying the flame characteristic, it is important to distinguish the flame types, which include premixed flame and non-premixed flame. In the present work, the premixed flames are only focused on studying the flame properties of a given mixture. The premixed flames are also known as combustion waves with the attributes of waves, in particular the property of propagating in a direction normal to themselves at a constant speed [33]. They are also referred to as the combustion mode that takes place when fuel and oxidizer have been mixed prior to the burning process [34]. The flames can be laminar or turbulent, but it is also mentioned that the study of the detailed chemistry of laminar premixed flames will provide information which applies to practically all premixed flames, whether laminar or turbulent [35], [36]. The illustration of a flame propagating into the unburnt mixture from a duct containing a premixed mixture of fuel and oxidizer can be seen in Figure (2.2) as follow.

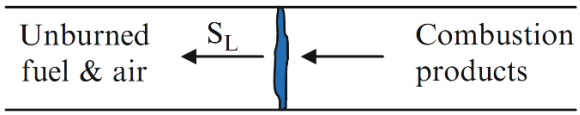

Figure 2.3. Premixed flame propagation from right to left [34]

The close-up view of the structure of the premixed flame propagation can also be illustrated as follow.

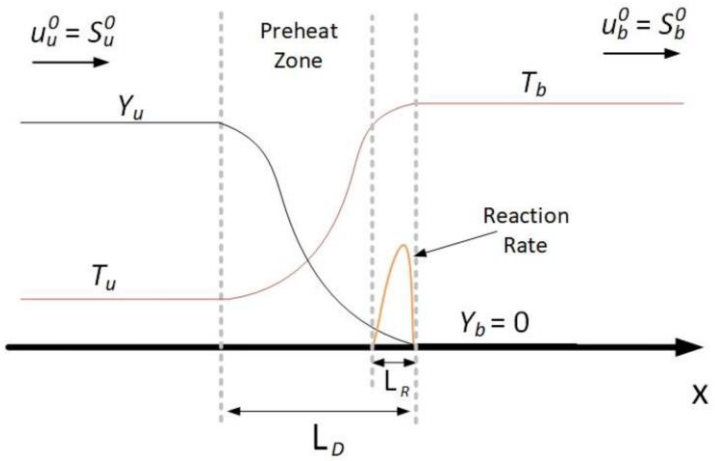

Figure 2.4. Detailed sketch of a premixed flame propagation [2]

In the process of premixed flame propagation, the chemical reactions become fast as the temperature of the reactant reaches the ignition temperature of the fuel. This, in turn, creates the combustion flame front. As fuel and oxidizer are consumed, the reaction rate decreases with the production of combustion products. The temperature of the products is observed to be close to the adiabatic flame temperature.

Flame propagation through the unburnt gas mixture depends on two consecutive processes. In the first process, the heat produced from the reaction heats the incoming unburnt mixture to the ignition temperature. Secondly, the preheated reactants chemically react in the reaction zone. Therefore, it is concluded that the flame speed will depend on both transport and chemical reaction properties [34].

Even though the flame properties such as propagation rates, heat release rates, flammability limits, quenching, and emissions can be determined analytically with the relevant formulas, some flame chemistry and characteristics can be observed with computer simulations with built-in complex chemical kinetic reaction schemes. According to the schemes, the burning velocities can be measured along with the propagation rate of a flame and the flame stretch.

The measurements of the flame speed will be discussed and described in a later chapter of the present work. However, detailed studies of transport properties and structure of premixed flames will not be elaborated according to the limit of the scope, and the handbook of "fundamentals of combustion processes" by Sara McAllister is recommended for detailed study.

2.4.2 Laminar burning velocity

Laminar burning velocity of a fuel and air mixture is defined in its one-dimensional configuration corresponding to the velocity at which the new premixed gases mixture makes a planar flame steady. While evaluating the laminar burning velocity, the flame has to be considered planar, one-dimensional, adiabatic, and unstretched according to the flame geometry of the burnt gases to achieve equilibrium. Generally, the laminar burning velocity is referred to as S_u^0 and depends on the initial conditions of pressure, temperature, and the chemical composition of the mixture. The laminar burning velocity is evaluated as it is

important in studying the combustion process regarding the reactivity, diffusivity, and exothermicity of a combustible mixture[33], [37], [38]. In addition, evaluating the laminar burning velocity is also important to validate the chemical kinetic mechanisms for conventional and alternative fuels and important in studying turbulent combustion modeling.

2.4.3 Stretched flames

Since laboratory flames are not planar and stretched flames, it is necessary to examine the stretch properties and unstretched flames corresponding to the flame velocities. The unstretched laminar burning velocity is the important characteristic of a given mixture, where analytical formulations calculate planar flame velocity from stretched flame velocity. Generally, there are three main stretched flame configurations as stagnation flame, spherical expanding flame, and bunsen burner flame to determine the laminar burning velocity [39]. Due to the range of scope, the spherical expanding flame configuration will be referred to in the present work.

In the spherical expanding flame technique, a homogeneous combustible mixture is ignited at the center of the vessel generating a propagating expanding flame. From the generated spherical flame, the radii with respect to time are obtained to find the flame speed using the constant volume method [33]. In this way, the flame speed and stretch rate are evaluated applying the approach mentioned above, and the stretch extrapolation technique is used to determine the unstretched laminar burning velocity from the stretched flame record. Using a linear stretched model along with evaluating the stretched and unstretched laminar burning velocities, the Markstein length can also be calculated to measure the sensitivity of the flame speed [27].

2.4.4 Chemical kinetic mechanism

Chemical kinetics is a branch of physical chemistry that focuses on understanding the rates of chemical reactions [20]. The rate of chemical process and continuous transformation of reactants to products for a certain mechanism is also defined using chemical kinetics. With the help of chemical kinetics, the chemical reaction for a specific mechanism can evaluate the process depending on different conditions. According to its complexity and structure, the evaluations of available detailed hydrogen/oxygen chemical kinetic mechanisms on the measurements of the properties of outwardly propagating laminar premixed flames of hydrogen proposed by Kim et al. [41], Yetter et al. [42], Mueller et al. [43], and Frenklach et al. [44] is also reviewed.

The detailed explanation regarding the derivations of flame equations, theories, chemical kinetic schemes, methods, and reaction mechanisms for hydrogen oxidation referred to in the present work can be elaborated in the literature “Burning velocity and the influence of flame stretch” by Simon Crispin Taylor [45].

2.4.5 Combustion of Hydrogen

Combustion is a chemical process in which energy is released from a fuel and air mixture. In hydrogen combustion, the gaseous hydrogen is burnt in a combustion vessel or specified combustion engines. Hydrogen can be combusted in a wide range of fuel-air mixtures for its wide flammability range. Hydrogen can also be observed that it can run on a lean mixture where the amount of fuel (hydrogen) is less than the amount of air needed for the combustion process [35].

As another feature of hydrogen, hydrogen has a high auto-ignition temperature, which enables higher compression ratios compared to different carbon fuels. Since the combustion of hydrogen in the air produces water, it avoids carbon-based pollution more than carbon fuels. Therefore, hydrogen becomes the most promising fuel to replace hydrocarbon fuels maintaining high efficiency in combustion systems despite its explosive characteristics. Moreover, safety aspects and development of hydrogen technology are being studied and carried out. In the present work, the laminar burning velocity of hydrogen, nitrogen, and oxygen mixture is evaluated to study the characteristic of propagating flames.

3 Experimental setups and procedure

In this chapter, the setup used for experiments and detailed procedures carried out during the experiments are described. From the setup, each piece of equipment utilized in the system is also presented with its brief function.

3.1 Experimental setup

The experimental setup consists of a combustion vessel with temperature and pressure sensors, a heating system, a gas supply system, controller systems, and a high-speed video camera to record propagating flames. The schematic experimental setup used in the present study can be seen in Figure (3.1).

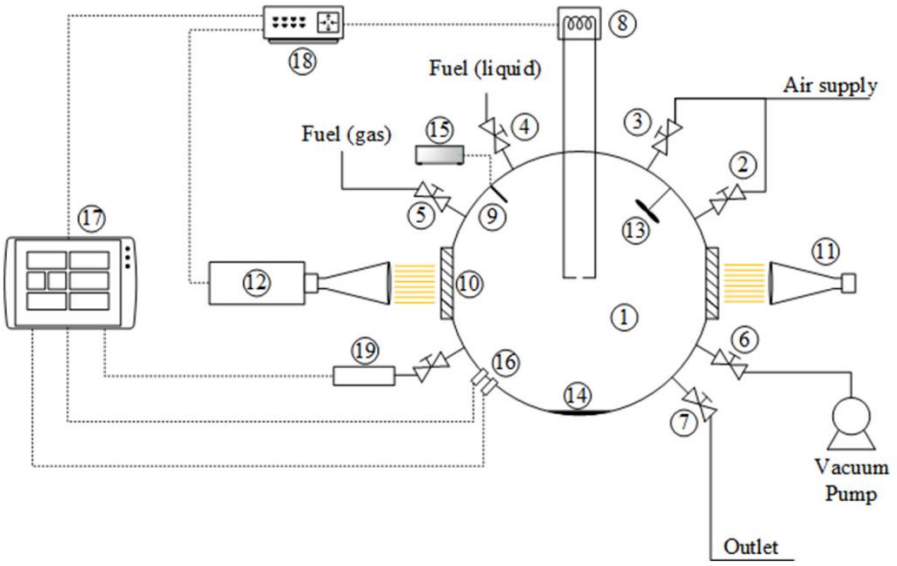

Figure 3.1. Schematic experimental setup [46]. 1: explosion chamber; 2: oxidizer inlet; 3: flush inlet; 4: fuel (liquid) injection port; 5: fuel (gas) inlet; 6: vacuum port; 7: gas outlet; 8: ignition system; 9: thermocouple; 10: glass windows (100mm); 11: LED light source; 12: high-speed video camera; 13: stirrer; 14: heating plate; 15: ambient temperature display; 16: dual explosion pressure sensors; 17: data acquisition system; 18: control/trigger unit and 19: ambient pressure sensor.

The experiments were carried out in a 20-liter explosion sphere with a constant volume combustion chamber with an internal volume of 20.4 dm^3. The vessel is insulated by a heating jacket from the outer chamber to avoid significant heat loss. There is a heating plate with a seperate temperature controller at the bottom of the vessel for evaporating liquids. The temperature of the combustion vessel and the gas temperature is measured using built-in temperature sensors and monitored with a separate display units of the combustion vessel. The combustible mixture quantities are prepared with the required partial pressure for each component by monitoring and recording the pressure with pressure transducers in an ambient pressure logger. The measured pressure values are displayed with computer-assisted software

and with oscilloscopes. There are three different inlet ports that allow liquid fuel, gaseous fuel, or oxidizer to fill up the vessel. A motorized fan is located inside the vessel to stir the ambient gas mixture to achieve a homogeneous mixture before ignition. The operating systems such as vacuum pump, stirrer, and fume extractor are operated with the controller from the separate control system of the combustion vessel.

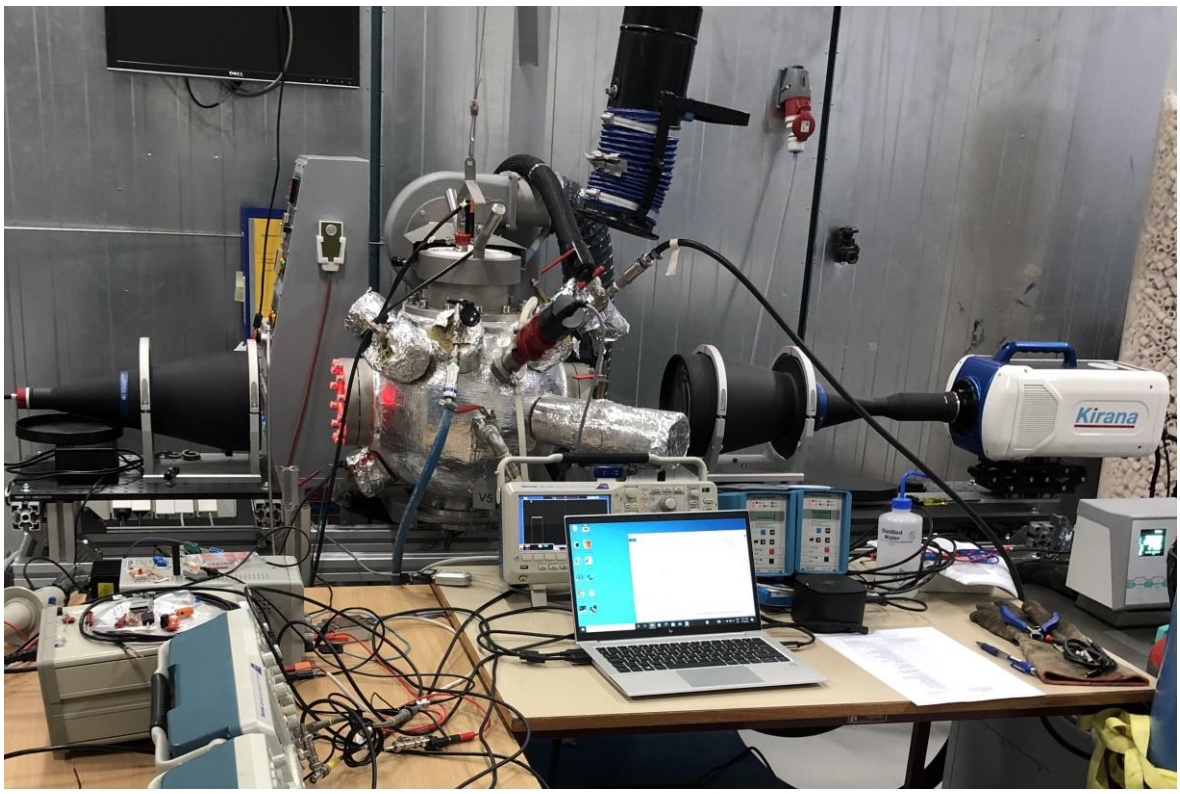

Figure 3.2. Setup of a 20-liter explosion vessel with data acquisition system

There is two oppositely faced circular windows of 100 mm in diameter providing optical access to the chamber. Through the windows, the flame propagation was recorded via the optical access of the chamber with the focused shadowgraph imaging technique and KIRANA ultra-high-speed video camera in the range from 1000 to 50 000 frames per second (fps) during the explosion. The images are achieved using a high-speed video camera with a telecentric lens and a lamp that emits collimated light, as can be seen in Figures (3.3) and (3.4).

Figure 3.3. KIRANA ultra-high-speed video camera with telecentric lens

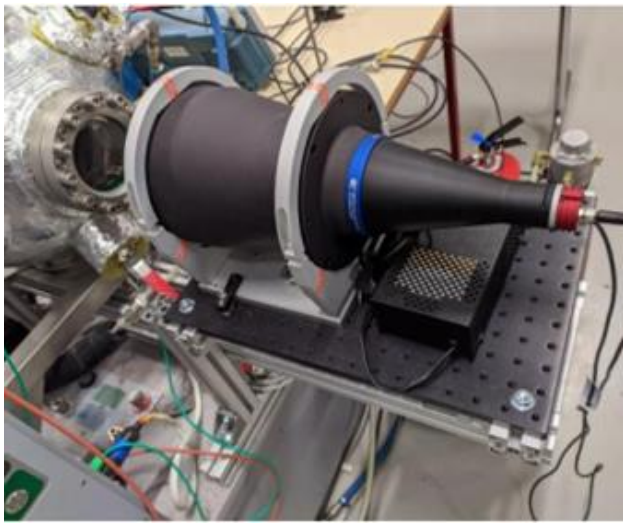

Figure 3.4. Collimated LED light source

The mixtures are ignited with a relevant ignition system at the center of the vessel aligned with the optical windows. There are two types of ignition systems ignition/exploding wire and electrical spark. In the present study, the capacitor discharge spark ignition system was used for the ignition wire, which is only used for high energy demanding explosion experiments. The electrostatic energy of a single spark charged in the capacitor was set, and the gas mixture was ignited.

After the explosion test, the final images from flame propagation can be generated via computer-assisted software. The explosion pressure inside the chamber during flame propagation is measured with pressure transducers and recorded with the ambient pressure logger and specified oscilloscopes. The rest of the output data, such as temperature, current, and voltage, can also be obtained by using temperature sensors, and oscilloscopes, respectively.

3.2 Experimental procedure

As the first step, all safety precautions were carried out, and gas cylinders were prepared. The explosion sphere was started, and a heating system was initiated for the vessel temperature varied a little depending on room temperature and the amount of heat transfer from previous experiments. While running the heating system, the camera and lamp were started to be ready for recording. As the vessel temperature reached the required temperature, the ambient pressure logger was turned on to monitor the pressure inside the vessel. The concentration targets of the gas mixture were prepared while purging with compressed oil-free air for about five minutes. After purging, the prepared fuel, nitrogen, and oxidizer were filled separately until their desired partial pressures with the right concentration. The nitrogen, oxidizer, and fuel were mixed and stirred with a mechanical stirrer inside the chamber for five minutes to get a homogeneous gas mixture before the mixture was ignited. The vessel temperature was recorded and noted after the mixing process. To ensure the mixture was quiescent, the ignition was delayed for three

minutes. After all these steps, the power source and supply for the ignition system, camera, and oscilloscope were prepared for ignition and explosion. Before ignition process, the ignition energies were also checked and recorded. By varying the capacitor charging in the ignition circuit to different voltages, the required ignition energy was set. For the image recordings, the camera speed was set in the range between 10 000 and 50 000 frames per second (fps) depending on the generated frames of the mixtures which is also decribed in the appendix section.

The ignition system was triggered for the explosion, then, data outputs were recorded and saved with computer-aided camera software and oscilloscopes accordingly to the experimental numbers. As the last step, the burnt residual gas was flushed with a fume extractor for five minutes to ensure the unnecessary gases were not trapped in the vessel before new experiments could be started.

4 Methodology

4.1 Evaluating the laminar burning velocity

The outwardly propagating spherical flame method was applied to determine the laminar flame speed. From the recorded images, the temporal evolution of the radius was measured using a developed image processing code in Python to analyze the digital images. As the first step of algorithms, the background from the generated images was subtracted, and all negative pixel values were set to zero. To distinguish the flame from the background, the threshold was set, and all pixels were stored above the set threshold. Furthermore, the outer perimeters were observed with removed outliers. Then, the radii of flames from images were produced by curve-fitting on the outer perimeter of the circle. In this way, the required radii with respect to time were obtained to evaluate the laminar burning velocity. The illustration of flame expanding with respect to time can be seen in Figure (4.1).

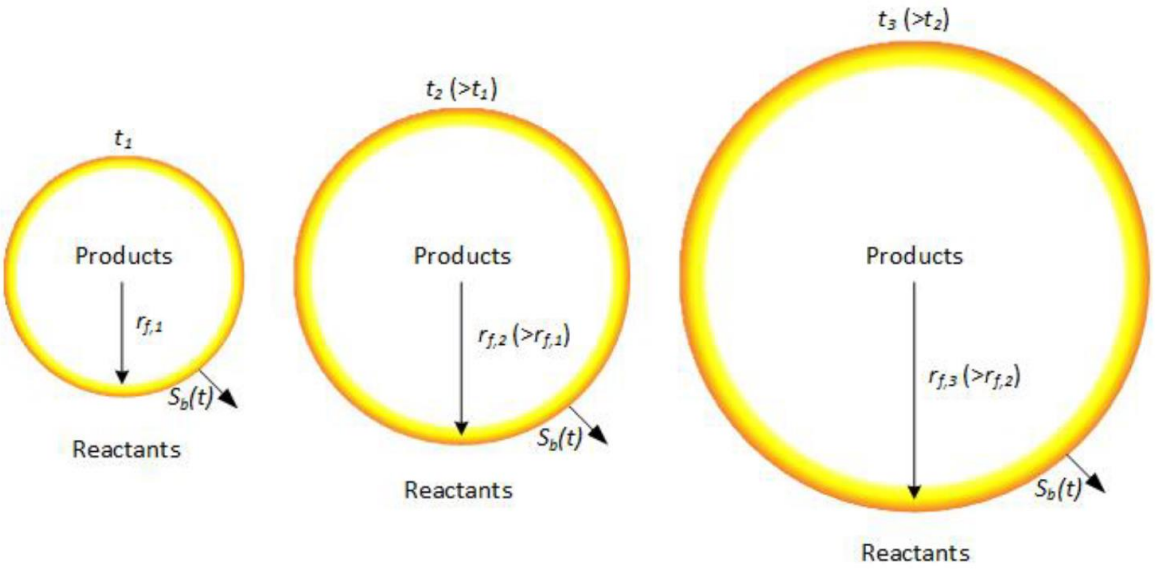

Figure 4.1. Illustration of spherical flame propagation with respect to time [2]

The generated radius-time record of flames can be used to derive the laminar flame speed as in Equation (4);

$$S_b = \frac{dr}{dt} \tag{4}$$

where r is the radius of the flame and t is time. Applying the linear stretch model curve fitting on the calculated flame speed and radius, the Markstein length (L_b) and the laminar flame speed (S_b^0) can be evaluated. Therefore, the laminar flame speed of the spherical flame is found to be dependent on the flame stretch rate. The relation between the laminar flame speed and the flame stretch rate can also be found in Equation (5);

$$\kappa = \frac{1}{A_f} \cdot \frac{dA_f}{dt} = \frac{2S_b}{r_f} \quad (5)$$

where A_f is the area of the spherical flame front. From the measured results, the unstretched flame speed could be calculated.

The data obtained from each mixture included a series of stretch rates with laminar flame speeds. By using the linear stretch model, the values of one-dimension laminar burning velocity and Markstein length could be calculated for each data set by extrapolating the stretch rate to zero and applying linear regression. From these techniques, the laminar burning velocity was observed as the intercept of the line and the Markstein length as minus the slope of the line. The laminar burning velocity (LBV) can be evaluated with the assumption of equilibrium between the unburnt and burnt conditions.

4.2 Calculation of mole fraction and partial pressure

While determining the mole fraction and partial pressure of the gas mixture, the combustion stoichiometry for general hydrocarbon fuel, $C_\alpha H_\beta O_\Upsilon$ is applied as the initial approach. It can be expressed as

$$C_\alpha H_\beta O_\Upsilon + (\alpha+\beta/4-\Upsilon/2)\ (O_2 + 3.76N_2) \rightarrow \alpha CO_2 + (\beta/2)\ H_2O + 3.76(\alpha+\beta/4-\Upsilon/2)\ N_2 \quad (6)$$

$$H_2 + (1/2)\ (O_2 + 3.76N_2) \rightarrow H_2O + 3.76(1/2)\ N_2 \quad (7)$$

$$2\phi H_2 + \lambda\ (O_2 + (1/\lambda)\ (4.76 - \lambda)\ N_2) \rightarrow \quad (8)$$

For $\phi = 1$ and $\lambda = 1$,

The reaction equation becomes

$$2H_2 + (O_2 + 3.76N_2) \rightarrow 2H_2O + 3.76N_2 \quad (9)$$

The equivalence ratio is a normalized quantity which provides the information of the content of the combustion mixture. For an alternative variable, air-fuel-ratio (AFR) is also called lambda (λ). Lambda is the actual air-fuel ratio to the stoichiometric air-fuel ratio defined as

$$\lambda = AFR/AFR_s = 1/\phi \quad (10)$$

Lambda of stoichiometric mixtures is 1. For rich mixtures, lambda is less than 1; for lean mixtures, lambda is greater than 1.

Moreover, mole fraction of each element can be calculated as follow.

$X_{H2} = 2/(2+4.76) = 0.2958$ (29.58%)

$X_{O2} = 1/6.76 = 0.1479$ (14.79%)

$X_{N2} = 3.76/6.76 = 0.5563$ (55.63%)

The partial pressure of any gas in a mixture is the total pressure multiplied by the mole fraction of that gas.

The total pressure is assumed to be 1000 mbar. Therefore, the partial pressure for H_2 would be (0.2958 x 1000 mbar = 296 mbar) and 148 mbar for O_2 and 556 mbar for N_2.

Following the same steps, the mole fractions and partial pressure for different ϕ and λ values are calculated. The calculated values are shown in Tables (4.1), (4.2), (4.3), and (4.4).

Table 4.1. Mole fractions of hydrogen, oxygen, and nitrogen with lambda from 0.3 to 1 at Phi = 1

Lambda	H2	O2	N2	N2/O2	O2/N2
1	29.59	14.79	55.62	3.76	0.27
0.8	29.59	11.83	58.58	4.95	0.20
0.6	29.59	8.88	61.54	6.93	0.14
0.5	29.59	7.40	63.02	8.52	0.12
0.4	29.59	5.92	64.50	10.90	0.09
0.3	29.59	4.44	65.98	14.87	0.07

Table 4.2. The required partial pressure of hydrogen, oxygen, and nitrogen to fill the vessel at lambda from 0.3 to 1

	H2[mbar]	Air[mbar]	N2[mbar]	Lambda	Phi
Partial pressure	296	704	0	1	1.00
Partial pressure	296	563	141	0.8	1.25
Partial pressure	296	422	282	0.6	1.67
Partial pressure	296	352	352	0.5	2.00
Partial pressure	296	282	422	0.4	2.50
Partial pressure	296	211	493	0.3	3.33

Table 4.3. Mole fractions of hydrogen, oxygen, and nitrogen with lambda from 0.3 to 1 at Phi = 0.8

Lambda	H2	O2	N2	N2/O2	O2/N2
1	25.16	15.72	59.12	3.76	0.27
0.8	25.16	12.58	62.26	4.95	0.20
0.6	25.16	9.43	65.41	6.93	0.14
0.5	25.16	7.86	66.98	8.52	0.12
0.4	25.16	6.29	68.55	10.90	0.09
0.3	25.16	4.72	70.13	14.87	0.07

Table 4.4. The required partial pressure of hydrogen, oxygen, and nitrogen to fill the vessel at lambda from 0.3 to 1

	H2[mbar]	Air[mbar]	N2[mbar]	Lambda	Phi
Partial pressure	252	748	0	1	1.00
Partial pressure	252	599	150	0.8	1.25
Partial pressure	252	449	299	0.6	1.67
Partial pressure	252	374	374	0.5	2.00
Partial pressure	252	299	449	0.4	2.50
Partial pressure	252	225	524	0.3	3.33

4.3 Cantera

Cantera is an open-source, object-oriented software tool developed and integrated into programming software such as Python and MATLAB to solve the following problems.

- Thermodynamics
- Chemical kinetics
- Transport process
- Reactor networks
- One-dimensional flames
- Multiphase mixture
- Surface chemistry

Cantera also supports several different types of reactions, including several types of homogeneous reactions, surface reactions, and electrochemical reactions [14]. In the present study, it is used to determine complex chemical kinetics, transport properties, and, importantly laminar burning velocity of the gas mixture within the combustion process. With a given kinetic mechanism, gaseous composition over a range of equivalence ratios, temperature and pressure, Cantera can simulate freely propagating premixed hydrogen flat flame with multicomponent transport properties under one-dimensional flames. The thermodynamic equilibrium solver "equilibrate" was used in the present work to predict the closed volume explosion pressure. Furthermore, the "FreeFlame" routine was applied to calculate the laminar burning velocity (LBVs). With the significant performance of the tool, unseen potential problems can be investigated to compare with experimental observation.

4.4 Linear regression in Python

To forecast the results of required parameters using a set of predictors, linear regression is necessary to implement in the programming tools. In the present work, linear regression tools in Python software are used to predict the results of laminar burning velocity [47].

After plotting the required data such as radius, stretch rate, and flame speed from recorded high-speed videos and photos, linear regression is implemented in Python with the package **NumPy** which is a basic Python scientific package. In addition, the package **scikit-learn** is also introduced for preprocessing data and implementing regression.

Using **scikit-learn** package in Python for linear regression, the following general steps are taken:

- Importing the packages and classes.
  numpy, **LinearRegression** from **sklearn.linear_model**
- Providing data to work with.
  Stretch rate, flame speed
- Doing appropriate transformations.
  reshape((n,1))
- Creating a regression model.

reg = **LinearRegression()**

- Fitting the model with existing data.
  reg = **LinearRegression().fit(**Stretch rate, flame speed**)**
- Applying the model for predictions.
  flameSpeed_pred = **reg.predict**(stretchrate)
- Checking the results of model fitting to know whether the model is satisfactory.
  checking "**coefficient of determination**:", "**intercept**:", and "**slope**:".

Thereby, using the variables of stretch rate and flame speed as a set of predictors, the laminar burning velocity is forecasted and evaluated.

4.5 Data filtering in Python

The **Savitzky-Golay** filter is used in the present work with python programming to smooth raw data such as radius with respect to time generated from high-speed videos and photos. It is known as a low pass filter, where the input parameter of the original noisy data has to be set with the length of the filter window and the order of the polynomial function used to fit. In order to get rid of the unnecessary fluctuations from input data, successive data points are fitted with a polynomial function which minimizes the fitting error. Following the above procedure with iterating the data points, a new series of data points fitting the original signal is obtained.

The **Savitzky-Golay** filter can be applied with the function **savgol_filter()** from the **scipy.signal** package [48]. In the function, the input array to filter, the window size used in the iteration for smoothing the signal, and the order of polynomial function used to fit the original dataset are used as the input variables, which can be seen as follows.

Signal = savgol_filter(input data, window_length, polyorder)

Where,

input data: the data to be filtered,

window_length: the length of the filter window which must be a positive odd integer less than the number of input data

polyorder: the order of the polynomial used to fit the samples. It must be less than the quantity of window_length

5 Results

5.1 Introduction

In the following section, the experimental results obtained with the experimental setup and procedure described in Chapter 3 are presented and discussed.

For the gas mixture of hydrogen, nitrogen, and oxygen with different fuel-air equivalence ratios and air-fuel equivalence ratios, the total number of sixty-six experiments were performed. In the experiments, three different fuel-air equivalence ratios (such as 1, 0.8, 0.6) with respect to five different air-fuel equivalence ratios (such as 1.0, 0.8, 0.6, 0.5, 0.4) were set to perform the experiments. Even though several tests were done, only a few experiments delivered the satisfying results due to the incorrect mixture and concentration of the gases and hydrodynamic instabilities. In addition, the setting of the high-speed video camera and ignition source was also observed to be important in achieving good results. Therefore, from the accurate experimental results at 300 K and 100 kPa, the required laminar burning velocity (LBVs), laminar flame speed, and Markstein length were determined for hydrogen, nitrogen, and oxygen mixture, which are elaborated in the following section.

After evaluating the experimental results, the predicted laminar burning velocity (LBVs) and laminar flame speed were calculated using Cantera to compare to the experimental results and to validate the experimental method.

5.2 Results and Discussion

In some experiments, the propagation of flame was influenced by Thermal diffusion, hydrodynamic instabilities, and buoyancy during explosion [2]. Although small instabilities were detected in some experiments, they were ignored where there were still spherical flame propagations at the beginning or at the end of the explosion.

The linear stretch extrapolations model, as mentioned in Table (2.1), was used in the present study to evaluate the unstretched flame propagation speed from the experimental results. From the calculation of unstretched laminar burning velocity and flame speed, the results were compared with the ones calculated using Cantera. The comparison of the gas mixture with fuel-air equivalence ratio (ϕ=1) can be seen in Table (5.1) and Figure (5.1), which conclude the results and method acceptably.

Table 5.1. Results of the unstretched laminar flame speed, laminar burning velocity, and Markstein length at 300 K, and 100 kPa with $\phi = 1$

Air-Fuel Equivalence Ratio (lambda)	Laminar Flame Speed, S_b^0, [m/s]	Laminar Burning Velocity, S_u^0, [m/s]	Cantera-Laminar Burning Velocity, S_u^0, [m/s]
1.0	14.71	2.17	2.35
0.8	11.92	1.95	2.08
0.6	6.78	1.33	1.42
0.5	4.17	0.92	0.88
0.5	4.31	0.95	0.88
0.5	4.41	0.98	0.88

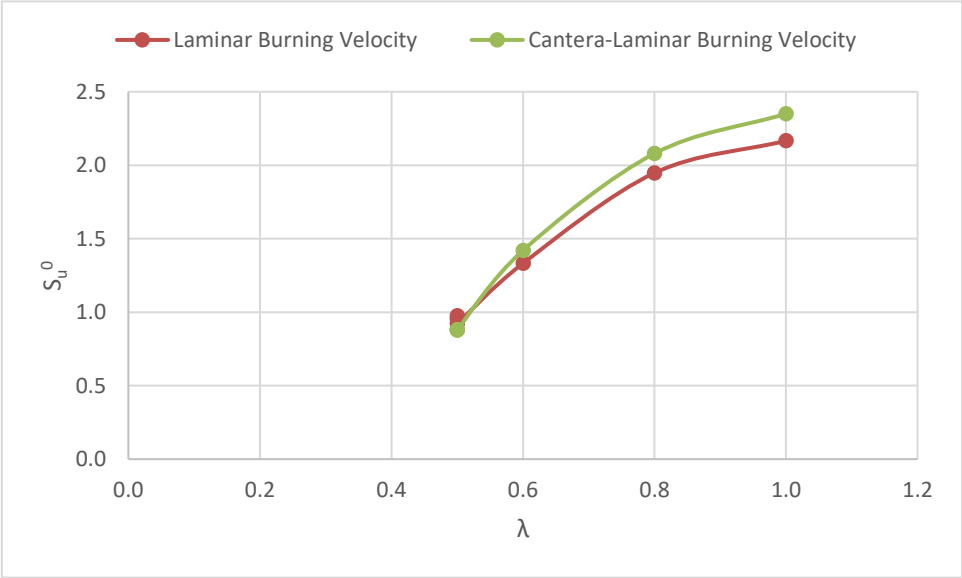

Figure 5.1. Comparison of experimental results and numerical results using Cantera

In figure (5.1), the laminar burning velocities at different air-fuel equivalence ratios are described and compared with the LBVs obtained using Cantera. The results show that the trend from the two datasets fits close enough even though only a few points at lambda (λ=0.5) overlap. The discrepancy between the experimental results and predicted simulation results from Cantera was concluded mainly due to the instabilities during flame propagation. However, the findings from the comparison indicated that the experimental setup and method produce acceptable results, which in turn validate the methods used in the present study. The illustration of spherical flame propagation at $\phi = 1$ and $\lambda = 0.5$ can be seen in Figure (5.3), where the radii with respect to time expanded correspondingly, giving the expected results.

The comparison of laminar burning velocities corresponding to the oxygen content in the oxidizer, $O_2/(O_2+N_2)$ from Figure (2.1) and Figure (5.1) at phi = 1 which is close to the one used in the literature study with phi = 1.058 from Chapter (2.1) is made. However, the value of oxygen content in the oxidizer of 0.1 from Figure (2.1) is only valid to compare with the

laminar burning velocity at lambda value of 0.5 (equal to 0.1 of $O_2/(O_2+N_2)$) from Figure (5.1). The comparison of laminar burning velocities at lambda of 0.5 can be found in Figure (5.2).

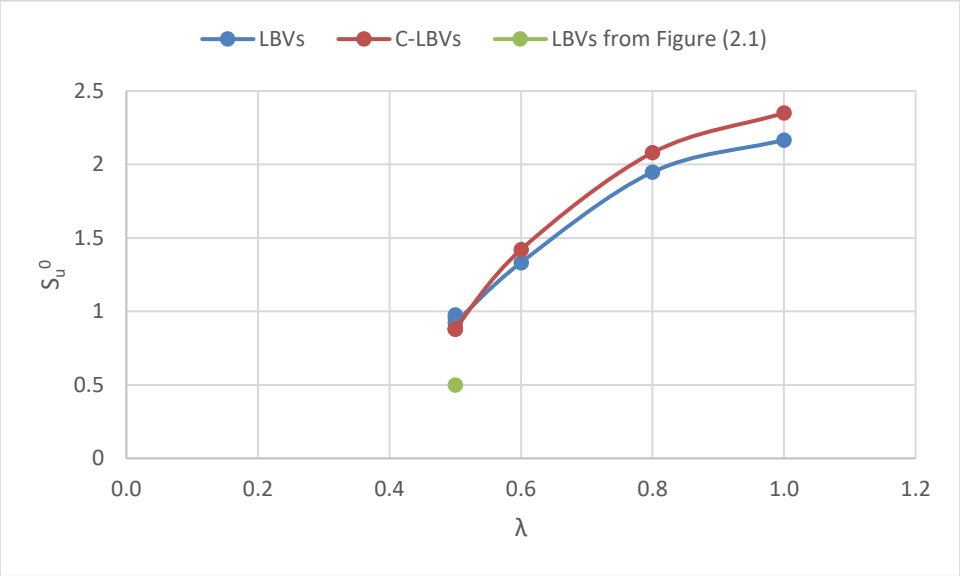

Figure 5.2. Comparison of experimental results and numerical results using Cantera with a value from literature study. LBVs (blue line with dots), laminar burning velocity from experiments; C-LBVs (red line with dots), laminar burning velocity calculated from CANTERA; LBVs (green dot), laminar burning velocity at oxygen content in the oxidizer of 0.1 which is equal to lambda of 0.5.

From the comparison, it is found that the values obtained from the present work is higher than the value from the literature. The deviation might be because of inaccurate values of phi which are 1 from the present work and 1.058 from the literature study. Moreover, it is also concluded that the laminar burning velocities from the present experimental test are higher for the newer experimental setups and technique are being used where less disturbances and losses are observed.

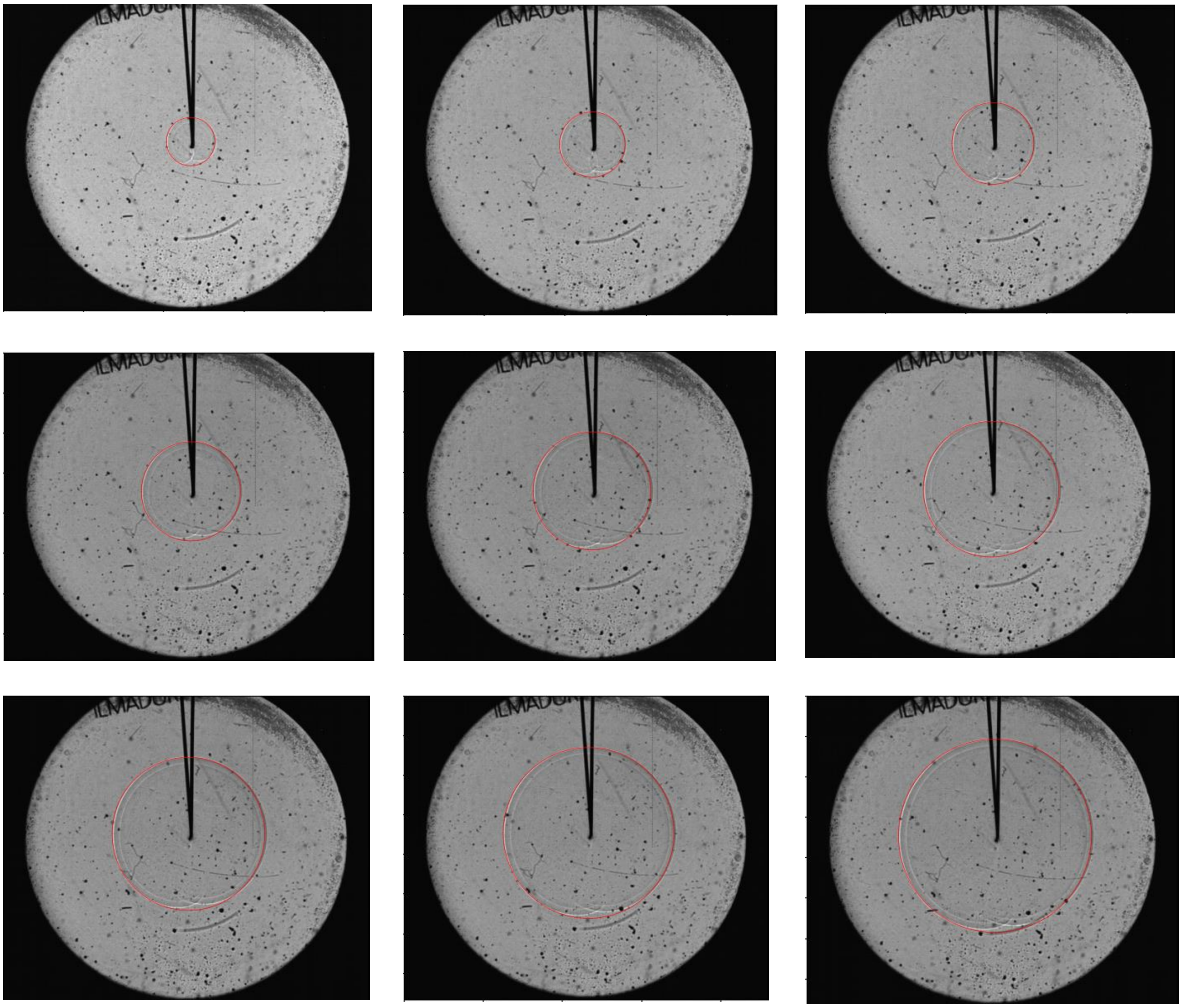

Figure 5.3. Illustration of captured spherical flame propagation from the experimental test with $\phi = 1, \lambda = 0.5$

After carrying out the experiments with fuel-air equivalence ratio (ϕ=1), the fuel and oxidizer concentrations were changed with fuel-air equivalence ratio (ϕ=0.8) to ensure the methods, theory, and setup used in the present work fit quite well with simulation and to study the behaviors in the explosion of lean hydrogen in hydrogen, nitrogen, and oxygen mixture.

The experiments were performed following the same procedure as in previous experiments with a fuel-air equivalence ratio (ϕ=1) with different air-fuel equivalence ratios (λ). As mentioned in the introduction part, only a few experiments were able to analyze because of no ignition. The observed data from the experiment with respect to air-fuel equivalence ratios are shown in Table (5.2) and Figure (5.4).

Table 5.2. Results of the unstretched laminar flame speed, laminar burning velocity, and Markstein length at 300 K, and 100 kPa with $\phi = 0.8$

Air-Fuel Equivalence Ratio (lambda)	Laminar Flame Speed, S_b^0, [m/s]	Laminar Burning Velocity, S_u^0, [m/s]	Cantera-Laminar Burning Velocity, S_u^0, [m/s]
1	4.02	0.64	1.66
0.8	1.29	0.21	2.08
0.5	2.27	0.48	0.93
0.4	0.04	0.01	0.42
0.4	0.22	0.05	0.42

The underlined numbers from Table (5.2) present the values which are significantly deviated from Cantera resultant values as it is illustrated in Figure (5.4).

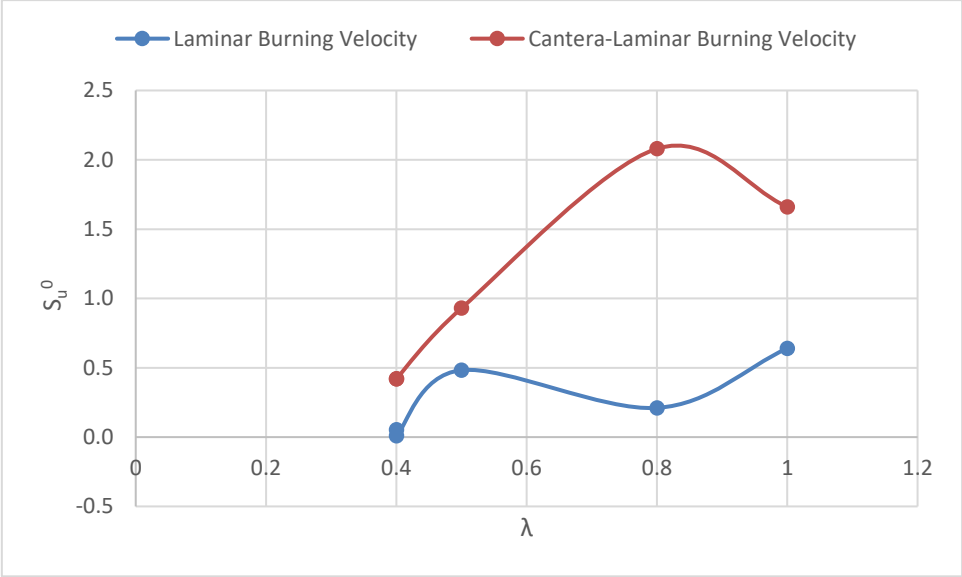

Figure 5.4. Comparison of experimental results and numerical results using Cantera

Figure (5.4) shows the trend of laminar burning velocity from experimental data and Cantera simulation. The datasets appear to be close at the lambda values of 0.4 and 0.5, but later from 0.8 to 1, the points from experiments and simulation deviate significantly. The investigations were also done to ensure the datasets were fitted well. However, the high-speed videos and images obtained from the experiment showed the irregular shapes of spherical flame propagation, which caused the image processing difficult to detect the flames. Since it is difficult to detect uniform flames, the linear stretch model could not handle the corresponding data to evaluate proper burning velocity. In these experiments, the flame radii with respect to time were fluctuated where constant flame propagation can be observed within a short time which cannot give desired data to determine laminar burning velocity. In some cases, the laminar flame speed is generated in negative values with positive Markstein length, which is not reasonable. As in one of the experiments, the flame did not propagate well enough to be

processed and utilized in evaluating laminar flame speed due to the inconsistent expansion of the flame, which is shown in Figure (5.5).

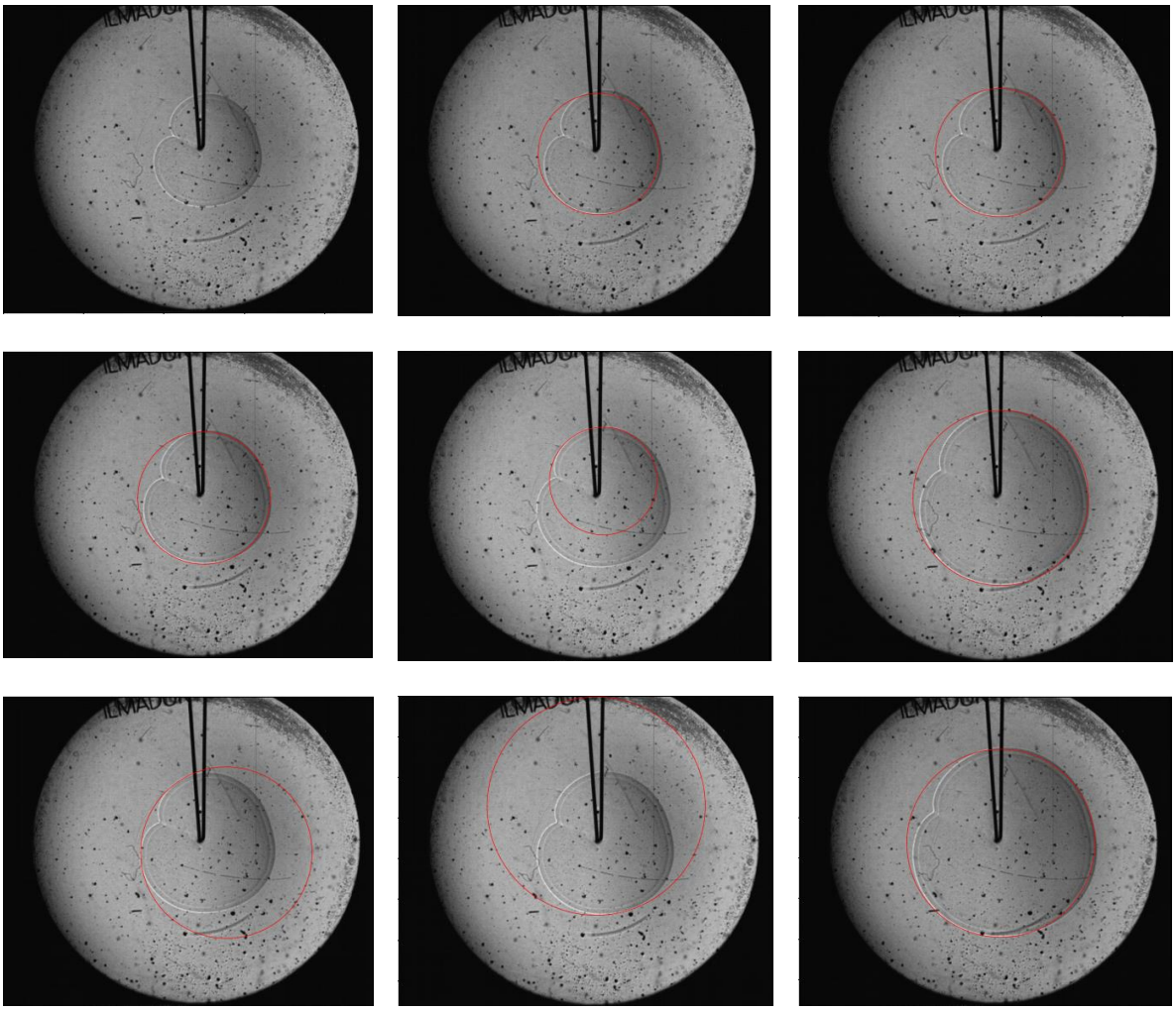

Figure 5.5. Illustration of captured spherical flame propagation from the experimental test with $\phi = 0.8, \lambda = 0.4$

To elaborate on the cause of two different cases in spherical flame propagation from Figure (5.3) and Figure (5.5), the comparison in flame radii developed during explosion with respect to time of regular and irregular flame shape is shown in Figure (5.6) and Figure (5.7).

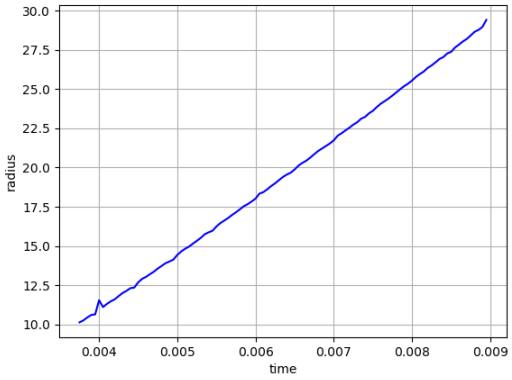

Figure 5.6. Illustration of the flame radius with respect to time at $\phi = 1, \lambda = 0.5$

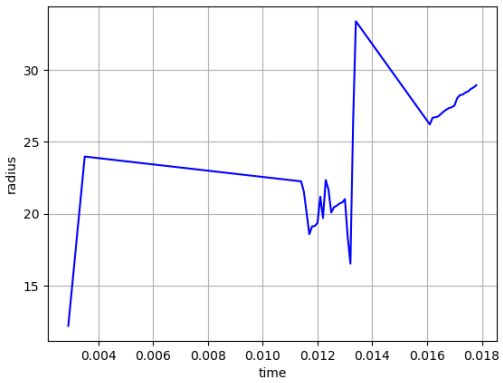

Figure 5.7. Illustration of the flame radius with respect to time at $\phi = 0.8, \lambda = 0.4$

In evaluating results such as laminar flame speed, coefficient of determination, and Markstein length, the linear stretched model described in Table (2.1) was used, generating the plot as shown in Figure (5.8) and Figure (5.9).

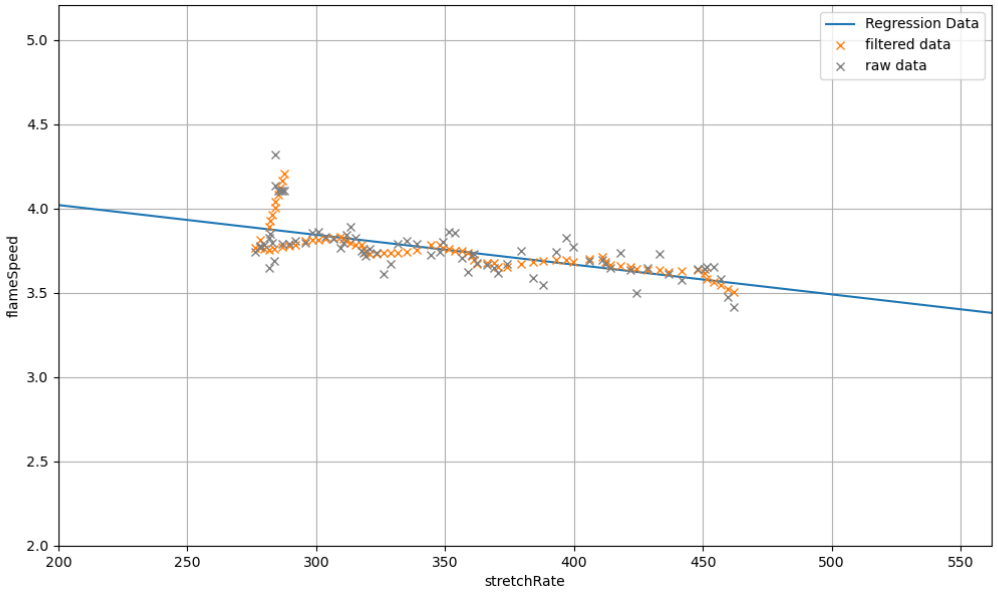

Figure 5.8. Plot showing resultant data from linear regression to determine required output data using linear stretch model ($\phi = 1, \lambda = 0.5$)

In Figure (5.8), the slope and data fitting on the regression line match the linear stretch model to produce laminar flame speed and Markstein length. In the case with $\phi = 1$ and $\lambda = 0.5$, the linear regression model gives positive laminar flame speed and negative Markstein length abiding the linear stretch model. However, in Figure (5.9), the slope can be seen as positive, which means the laminar flame speed will be negative and Marstein length in positive sign.

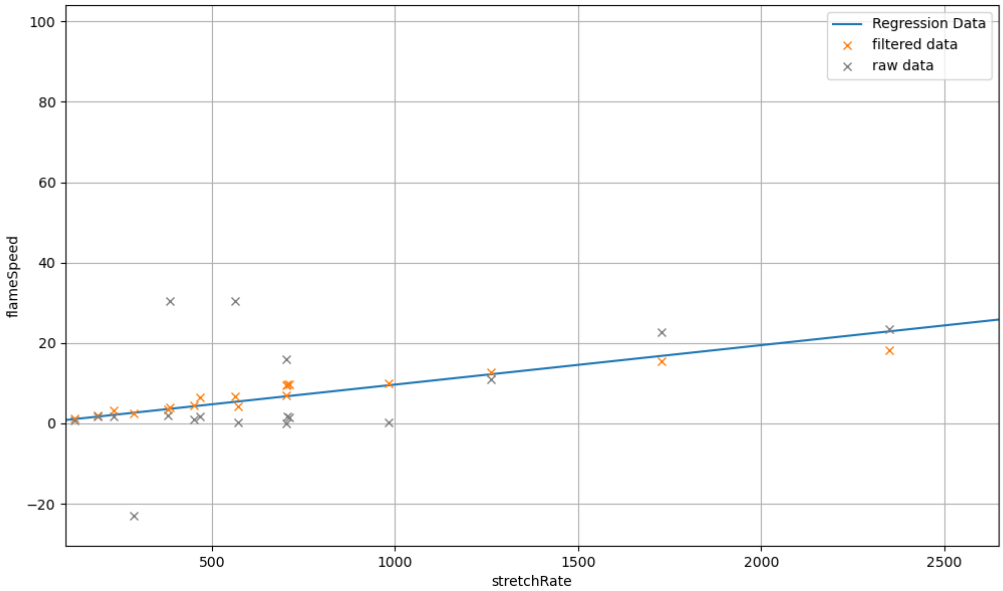

Figure 5.9. Plot showing resultant data from linear regression to determine required output data using linear stretch model ($\phi = 0.8$, $\lambda = 0.4$)

Therefore, it is concluded that the discrepancy between the experimental results and Cantera simulation results was due to the instabilities during the explosion and incorrect concentrations of each gas. According to the time restrictions on the present work, the factors influencing instabilities and causing errors could not review and redo experiments to produce better flame propagation.

6 Conclusion

The main aim of this study was to evaluate the laminar burning velocity of the hydrogen-oxygen-nitrogen mixture to investigate whether the hydrogen explosions can be mitigated by reducing oxygen concentration. To examine the effect of variations in oxygen concentrations, the laminar burning velocity of the mixture was determined.

The laminar flame speed, Markstein length, and laminar burning velocities of hydrogen-oxygen-nitrogen mixtures at different concentrations were determined from a closed vessel gas explosion of a 20-liter explosion sphere at the initial temperature of 300 K and the initial absolute pressure of 100 kPa.

Initially, quiescent mixtures were ignited in the explosion vessel. The images were captured with a high-speed video camera and processed with an image processing code [2] to extract the relevant combustion characteristics. The air-fuel equivalence ratio varied from 0.4 to 1 under the fuel-air equivalence ratio of 1 and 0.8. From experiments and the simulation tool "Cantera," nearly spherical outward propagating flames passing through homogeneous mixtures were investigated both experimentally and numerically. In the experiments, inaccuracies due to the flame curvature and flame acceleration caused by thermodynamic instabilities of the explosion were observed unexpectedly. Minor inaccuracies were rejected where there are proper sufficient flame propagations to determine flame speed. Besides the experimental work, numerical calculations with the Cantera simulation tool integrated into Python were also performed to compare the resulting laminar burning velocities from each approach. The conclusions from the comparison of experimental and numerical findings are described as follows:

- The results from hydrogen-rich mixtures give good results where explosion tests could be performed well. The hydrogen-rich mixtures with a fuel-air equivalence ratio of 1 delivered better results than the one with a fuel-air equivalence ratio of 0.8, which were interpreted and shown in Chapter 5. In addition, the results from the present work were also compared with the results from previous work done by Hermanns [5] illustrated in Figure (5.2).
- Under the hydrogen-rich mixture, the experiments with different air-fuel equivalence ratios were performed. The resulting laminar burning velocities of hydrogen-rich mixtures from experimental findings are found to be quite close to the results obtained from numerical calculations using Cantera. Small deviations were also observed in the results and were concluded to be due to minor loss of thermodynamic properties during the explosion.
- The hydrogen-lean mixtures with a fuel-air equivalence ratios of 0.8 give less accurate results where there are high discrepancies in each point of air-fuel equivalence ratios. For having high inaccuracies was also concluded to be the instabilities caused by changes in the thermodynamics of the unburnt mixture and inaccurate concentrations of fuel and oxidizer required for the explosion. Moreover, it is also concluded that more advanced methods might need to introduce in determining the laminar burning velocity.

To fulfill the aim of this study, the first scenario of the hydrogen-rich mixture can be taken to find the behavior of hydrogen explosion by examining the laminar burning velocity varying the oxygen concentration. In this case, the laminar burning velocities are increasing as the

oxygen concentration increases, where hydrogen concentration is kept constant. The illustration can be found in Figure (5.1).

Therefore, this study shows that the oxygen concentration in hydrogen explosion is important for safety purposes and developing hydrogen technology. While proving less oxygen concentration can mitigate hydrogen explosion, it is also validated that the experimental setup, technique, and methods used in this study are acceptable by comparing the results with simulation results from Cantera.

7 References

[1] F. N. Egolfopoulos, P. Cho, and C. K. Law, “Laminar flame speeds of methane-air mixtures under reduced and elevated pressures,” *Combust. Flame*, vol. 76, no. 3–4, pp. 375–391, Jun. 1989, doi: 10.1016/0010-2180(89)90119-3.

[2] M. Henriksen, *A study of premixed combustion of gas vented from failed Li-ion batteries*. University of South-Eastern Norway, 2021. Accessed: Apr. 29, 2022. [Online]. Available: https://openarchive.usn.no/usn-xmlui/handle/11250/2829351

[3] K. Bosschaart, “Detailed analysis of the heat flux method for measuring burning velocities,” *Combust. Flame*, vol. 132, no. 1–2, pp. 170–180, Jan. 2003, doi: 10.1016/S0010-2180(02)00433-9.

[4] M. Van A. (Arjen), “One-step chemical reaction parameters for premixed laminar flames,” 1994, doi: 10.6100/IR417400.

[5] R. T. E. Hermanns, A. A. Konnov, R. J. M. Bastiaans, and L. P. H. de Goey, “Laminar Burning Velocities of Diluted Hydrogen−Oxygen−Nitrogen Mixtures,” *Energy Fuels*, vol. 21, no. 4, pp. 1977–1981, Jul. 2007, doi: 10.1021/ef060553g.

[6] M. Henriksen, K. Vaagseather, A. V. Gaathaug, J. Lundberg, S. Forseth, and D. Bjerketvedt, “Laminar Burning Velocity of the Dimethyl Carbonate–Air Mixture Formed by the Li-Ion Electrolyte Solvent,” *Combust. Explos. Shock Waves*, vol. 56, no. 4, pp. 383–393, Aug. 2020, doi: 10.1134/S0010508220040024.

[7] C. K. Law, *Law. (2006). Combustion physics (pp. XVIII, 722). Cambridge University Press.*

[8] Z. Chen, “On the extraction of laminar flame speed and Markstein length from outwardly propagating spherical flames,” *Combust. Flame*, p. 10, 2011.

[9] F. A. Williams, *Combustion theory: the fundamental theory of chemically reacting flow systems*, 2nd ed. Menlo Park, Calif: Benjamin/Cummings Pub. Co, 1985.

[10] F. Wu, “Uncertainty in stretch extrapolation of laminar flame speed from expanding spherical flames,” *Proc. Combust. Inst.*, p. 8, 2015.

[11] Kelley, A., Bechtold, J., & Law, C., *Kelley, A., Bechtold, J., & Law, C. (2012). Premixed flame propagation in a confining vessel with weak pressure rise. Journal of Fluid Mechanics, 691, 26-51. doi:10.1017/jfm.2011.439.*

[12] A. P. Kelley and C. K. Law, “Nonlinear effects in the extraction of laminar flame speeds from expanding spherical flames,” *Combust. Flame*, vol. 156, no. 9, pp. 1844–1851, Sep. 2009, doi: 10.1016/j.combustflame.2009.04.004.

[13] Q. Liu, X. Chen, Y. Shen, and Y. Zhang, “Parameter extraction from spherically expanding flames propagated in hydrogen/air mixtures,” *Int. J. Hydrog. Energy*, vol. 44, no. 2, pp. 1227–1238, Jan. 2019, doi: 10.1016/j.ijhydene.2018.11.004.

[14] *Goodwin, D. G., Moffat, H. K., & Speth, R. L. (2016).* Cantera: An Object-Oriented Software Toolkit For Chemical Kinetics, Thermodynamics, And Transport Processes. Version 2.2.1. *Zenodo. https://doi.org/10.5281/ZENODO.45206*.

[15] B. Lewis and G. von Elbe, “Determination of the Speed of Flames and the Temperature Distribution in a Spherical Bomb from Time-Pressure Explosion Records,” *J. Chem. Phys.*, vol. 2, no. 5, pp. 283–290, May 1934, doi: 10.1063/1.1749464.

[16] G. K. Giannakopoulos, A. Gatzoulis, C. E. Frouzakis, M. Matalon, and A. G. Tomboulides, “Consistent definitions of ‘Flame Displacement Speed’ and ‘Markstein Length’ for premixed flame propagation,” *Combust. Flame*, vol. 162, no. 4, pp. 1249–1264, Apr. 2015, doi: 10.1016/j.combustflame.2014.10.015.

[17] P. Clavin, “Dynamic behavior of premixed flame fronts in laminar and turbulent flows,” *Prog. Energy Combust. Sci.*, vol. 11, no. 1, pp. 1–59, Jan. 1985, doi: 10.1016/0360-1285(85)90012-7.

[18] A. A. Konnov, A. Mohammad, V. R. Kishore, N. I. Kim, C. Prathap, and S. Kumar, “A comprehensive review of measurements and data analysis of laminar burning velocities for various fuel+air mixtures,” *Prog. Energy Combust. Sci.*, vol. 68, pp. 197–267, Sep. 2018, doi: 10.1016/j.pecs.2018.05.003.

[19] D. B. Spalding, P. L. Stephenson, and R. G. Taylor, “A calculation procedure for the prediction of laminar flame speeds,” *Combust. Flame*, vol. 17, no. 1, pp. 55–64, Aug. 1971, doi: 10.1016/S0010-2180(71)80138-4.

[20] P. L. Stephenson and R. G. Taylor, “Laminar flame propagation in hydrogen, oxygen, nitrogen mixtures,” *Combust. Flame*, vol. 20, no. 2, pp. 231–244, Apr. 1973, doi: 10.1016/S0010-2180(73)80177-4.

[21] J. Warnatz, “Calculation of the Structure of Laminar Flat Flames I: Flame Velocity of Freely Propagating Ozone Decomposition Flames,” *Berichte Bunsenges. Für Phys. Chem.*, vol. 82, no. 2, pp. 193–200, 1978, doi: 10.1002/bbpc.197800010.

[22] J. Warnatz, “The Structure of Freely Propagating and Burner-Stabilized Flames in the H2 - CO - O2 System,” *Berichte Bunsenges. Für Phys. Chem.*, vol. 83, no. 9, pp. 950–957, 1979, doi: 10.1002/bbpc.19790830915.

[23] “KeeRJ,GrcarJF,SmookeMD,MillerJA,MeeksE.PREMIX:afortranprogramformodelingsteadylaminarone-dimensionalpremixedflames.SandiaNationalLaboratoriesReport;1985(SAND85-8249).”.

[24] “KeeRJ,MillerJA,EvansGH,Dixon-LewisG.Acomputationalmodelofthestruc-tureandextinctionofstrained,opposedflow,premixedmethane-airflames.Symp(Int)Combust1988;22(1):1479–94.”.

[25] “Pitsch,H.,FlameMaster,aC++computerprogramfor0Dcombustionand1Dlaminarflame calculations.1998.”.

[26] “RoggB,W.W.RUN1DL:thelamianrflameandflamletcode.CambridgeUniver-sity;1995.”.

[27] “SomersL.Thesimulationofflatflameswithdetailedandreducedchemicalmodels.Eindhoven:EindhovenUniversityofTechnology;1994.”.

[28] “ChenZ,BurkeMP,JuY.EffectsofLewisnumberandignitionenergyonthedeterminationof

laminarflamespeedusingpropagatingsphericalflames.ProcCombustInst2009;32(1):1253–60.”.

[29] “CuociA,FrassoldatiA,FaravelliT,RanziE.OpenSMOKE++:Anobject-orientedframeworkforthenumericalmodelingofreactivesystemswithdetailedkineticmechanisms.ComputPhysCommun2015;192:237–64.”.

[30] “Padmanabha,R.,AGNISOFT.2016.”.

[31] G. H. Markstein, “Experimental and Theoretical Studies of Flame-Front Stability,” *J. Aeronaut. Sci.*, vol. 18, no. 3, pp. 199–209, Mar. 1951, doi: 10.2514/8.1900.

[32] A. E. Dahoe, “Laminar burning velocities of hydrogen–air mixtures from closed vessel gas explosions,” *J. Loss Prev. Process Ind.*, p. 15, 2005.

[33] E. Varea, “Experimental analysis of laminar spherically expanding flames,” p. 197.

[34] S. McAllister, J.-Y. Chen, and A. C. Fernandez-Pello, *Fundamentals of Combustion Processes*. New York, NY: Springer New York, 2011. doi: 10.1007/978-1-4419-7943-8.

[35] P. Pasiak, “COMPUTATION OF LAMINAR HYDROGEN FLAMES,” p. 50.

[36] L. Qiao, C. Kim, and G. Faeth, “Suppression effects of diluents on laminar premixed hydrogen/oxygen/nitrogen flames,” *Combust. Flame*, vol. 143, no. 1–2, pp. 79–96, Oct. 2005, doi: 10.1016/j.combustflame.2005.05.004.

[37] H. ErJiang, H. ZuoHua, H. JiaJia, J. Chun, M. HaiYan, and W. XiBin, “Measurement of laminar burning velocities and analysis of flame stabilities for hydrogen-air-diluent premixed mixtures,” vol. 54, no. 5, p. 12, 2009.

[38] Z. Huang, Y. Zhang, K. Zeng, B. Liu, Q. Wang, and D. Jiang, “Measurements of laminar burning velocities for natural gas–hydrogen–air mixtures,” *Combust. Flame*, vol. 146, no. 1–2, pp. 302–311, Jul. 2006, doi: 10.1016/j.combustflame.2006.03.003.

[39] X. Lu, “Experimental and kinetic study of laminar flame characteristics of H2/O2/diluent flame under elevated pressure,” *N T E R N T O N J O U R N O F H R O G E N E N E R G*, p. 13.

[40] T. Tahtouh, F. Halter, E. Samson, and C. Mounaïm-Rousselle, “Effects of hydrogen addition and nitrogen dilution on the laminar flame characteristics of premixed methane–air flames,” *Int. J. Hydrog. Energy*, vol. 34, no. 19, pp. 8329–8338, Oct. 2009, doi: 10.1016/j.ijhydene.2009.07.071.

[41] K. T. Aung, M. I. Hassan, and G. M. Faeth, “Flame stretch interactions of laminar premixed hydrogen/air flames at normal temperature and pressure,” *Combust. Flame*, vol. 109, no. 1, pp. 1–24, Apr. 1997, doi: 10.1016/S0010-2180(96)00151-4.

[42] R. A. Yetter, F. L. Dryer, and H. Rabitz, “A comprehensive reaction mechanism for carbon monoxide/hydrogen/oxygen kinetics,” *Combust. Sci. Technol.*, vol. 79, no. 1–3, pp. 97–128, Sep. 1991, doi: 10.1080/00102209108951759.

[43] M. A. Mueller, T. J. Kim, R. A. Yetter, and F. L. Dryer, “Flow reactor studies and kinetic modeling of the H2/O2 reaction,” *Int. J. Chem. Kinet.*, vol. 31, no. 2, pp. 113–125, 1999, doi: 10.1002/(SICI)1097-4601(1999)31:2<113::AID-KIN5>3.0.CO;2-0.

[44] W. C. Gardiner *et al.*, “The GRI-MechTM Model for Natural Gas Combustion and NO Formation and Removal Chemistry,” p. 3.

[45] S. C. Taylor, “Burning velocity and the influence of flame stretch,” phd, University of Leeds, 1991. Accessed: Apr. 28, 2022. [Online]. Available: https://etheses.whiterose.ac.uk/2099/

[46] M. Henriksen, K. Vaagsaether, J. Lundberg, S. Forseth, and D. Bjerketvedt, “Laminar burning velocity of gases vented from failed Li-ion batteries,” *J. Power Sources*, vol. 506, p. 230141, Sep. 2021, doi: 10.1016/j.jpowsour.2021.230141.

[47] R. Python, “Linear Regression in Python – Real Python.” https://realpython.com/linear-regression-in-python/ (accessed May 08, 2022).

[48] “scipy.signal.savgol_filter — SciPy v1.8.0 Manual.” https://docs.scipy.org/doc/scipy/reference/generated/scipy.signal.savgol_filter.html (accessed May 08, 2022).

8 Appendices

Appendix A: Experimental results from the test number (T12) where ignition was observed.

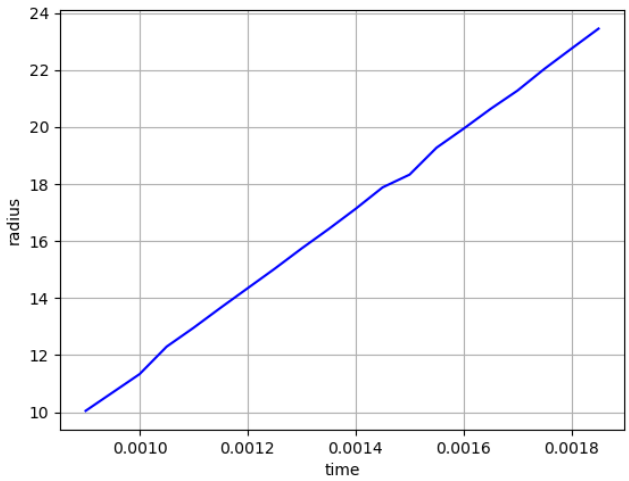

Figure A.1. Propagating flame radius with respect to time from Test 12

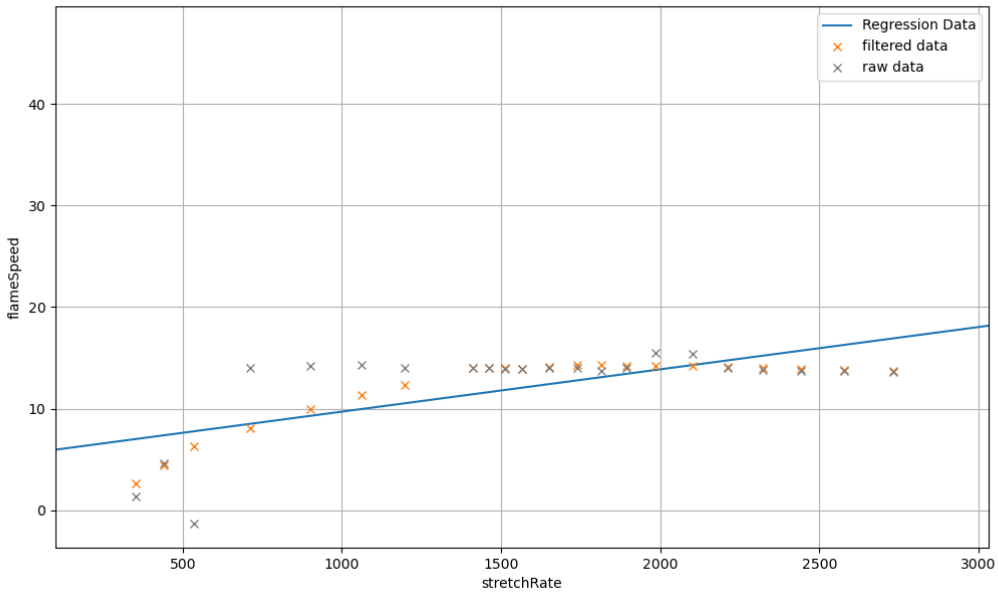

Figure A.2. Regression data, filtered data, and raw data to determine the flame speed with respect to stretch rate from Test 12

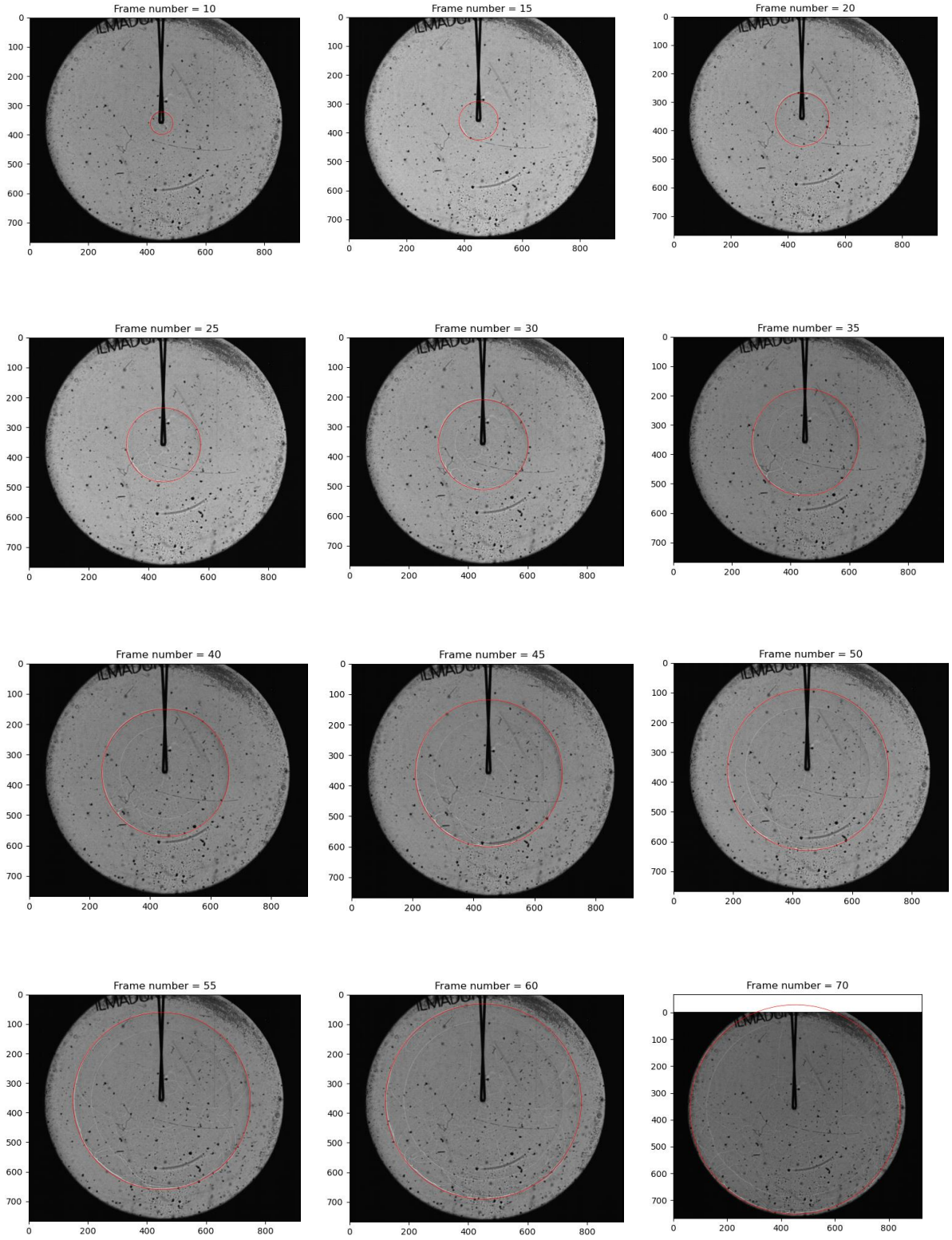

Figure A.3. Illustration on flame propagations at different frame numbers from Test 12

Appendix B: Experimental results from the test number (T13) where ignition was observed.

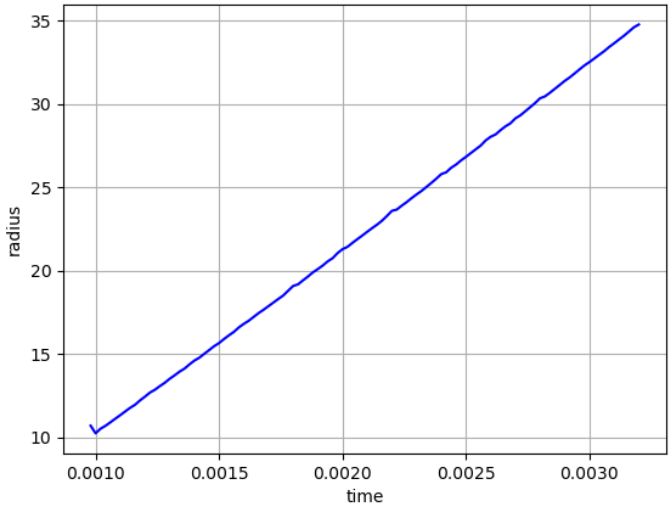

Figure B.1. Propagating flame radius with respect to time from Test 13

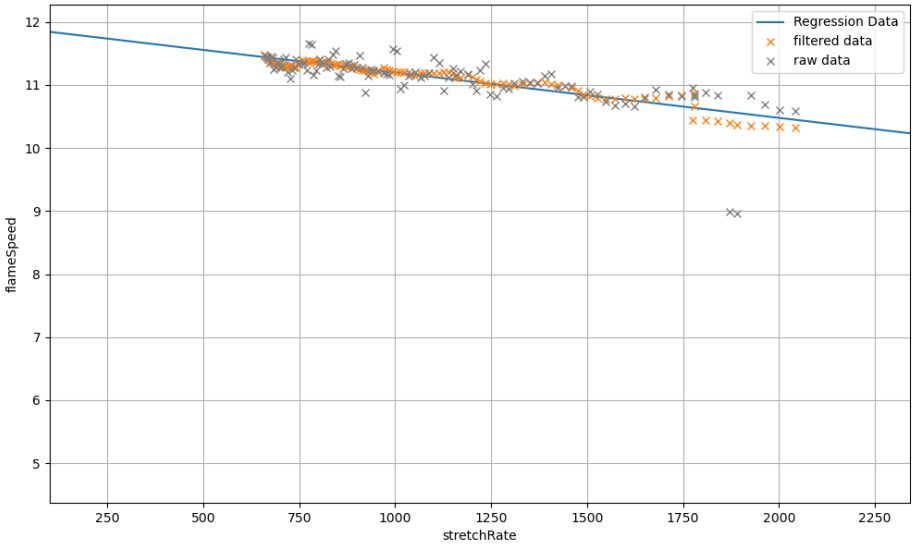

Figure B.2. Regression data, filtered data, and raw data to determine the flame speed with respect to stretch rate from Test 13

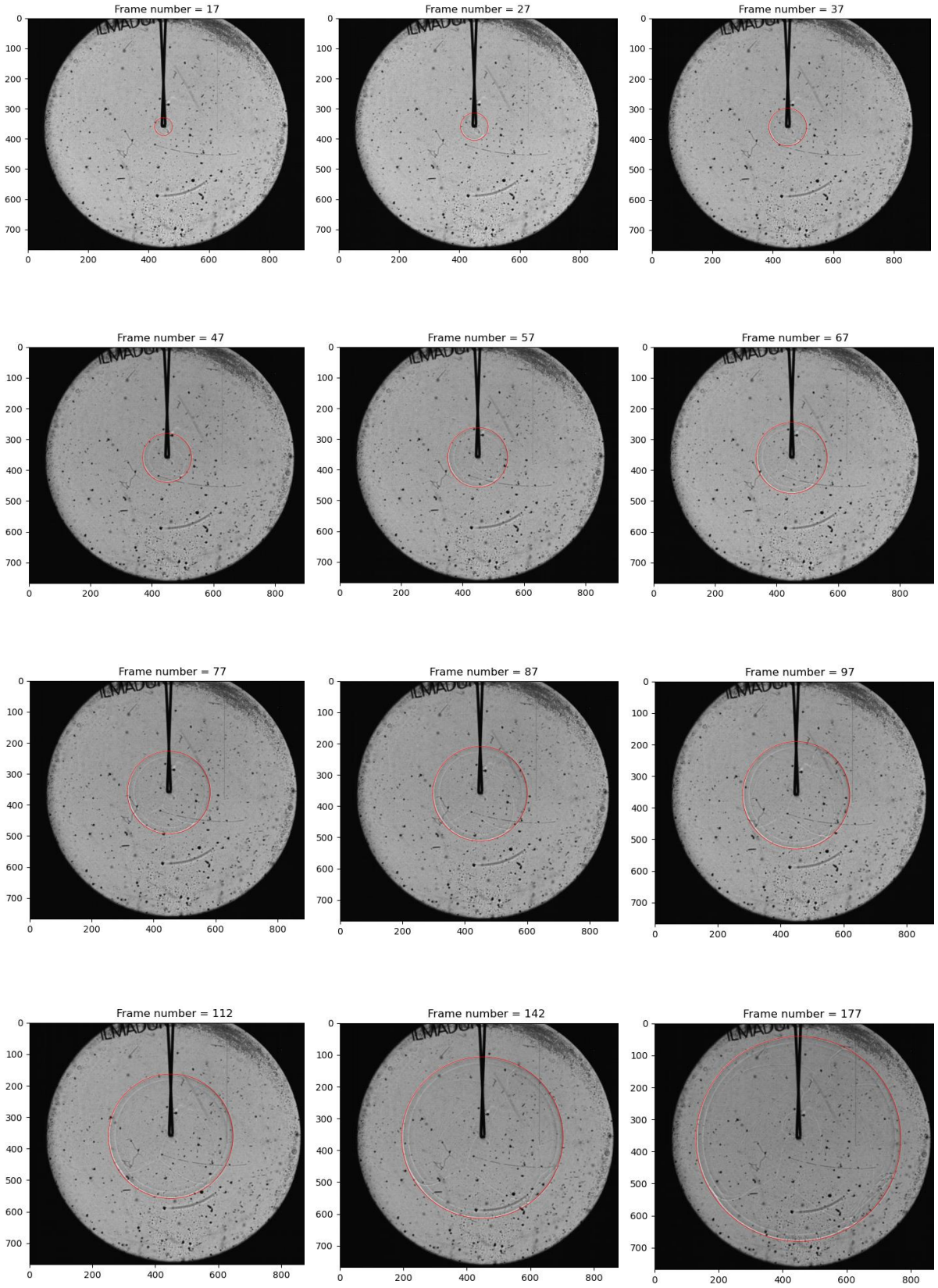

Figure B.3. Illustration on flame propagations at different frame numbers from Test 13

Appendix C: Experimental results from the test number (T14) where ignition was observed.

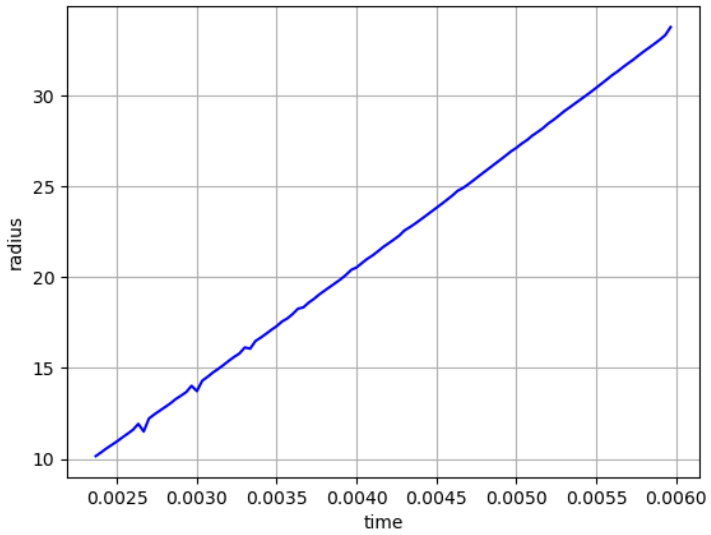

Figure C.1. Propagating flame radius with respect to time from Test 14

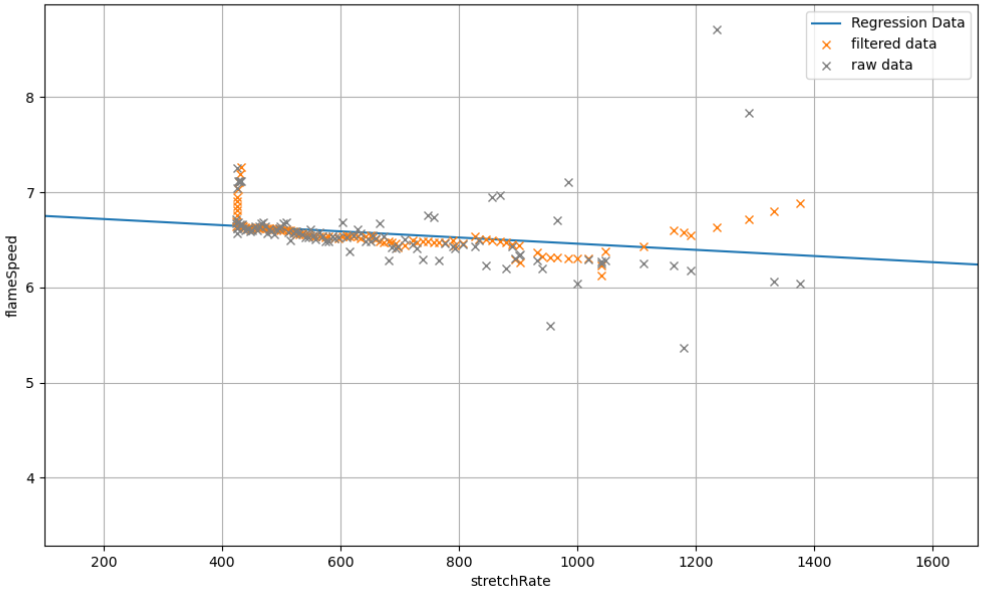

Figure C.2. Regression data, filtered data, and raw data to determine the flame speed with respect to stretch rate from Test 14

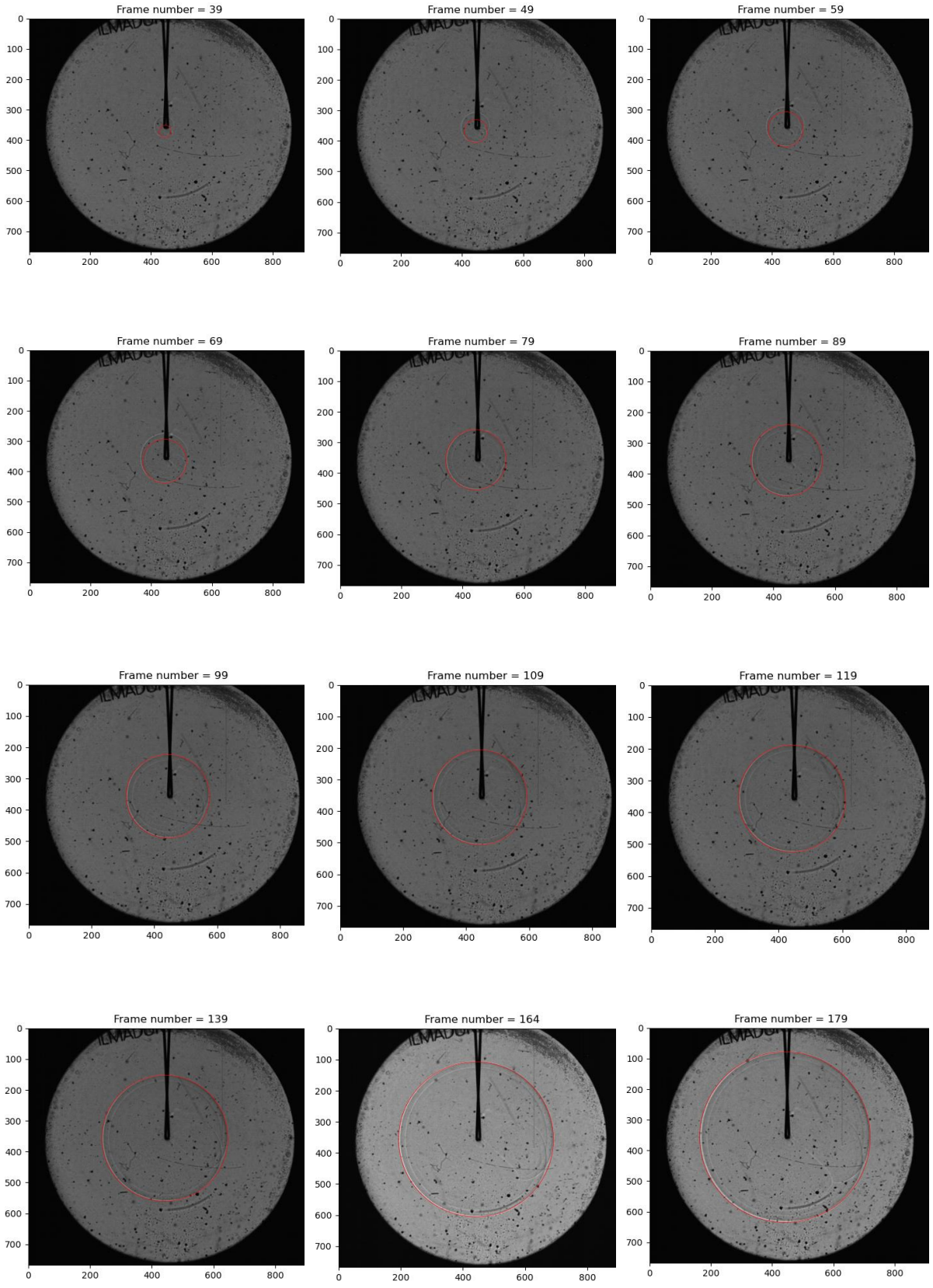

Figure C.3. Illustration on flame propagations at different frame numbers from Test 14

Appendix D: Experimental results from the test number (T36) where ignition was observed.

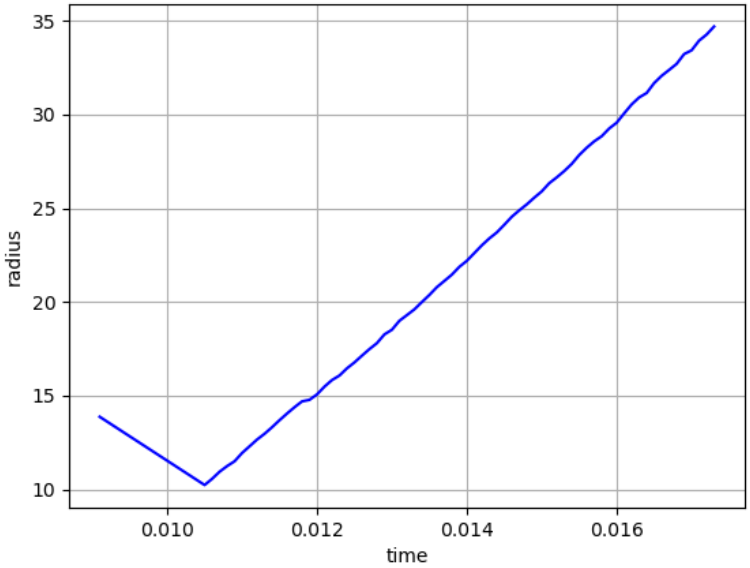

Figure D.1. Propagating flame radius with respect to time from Test 36

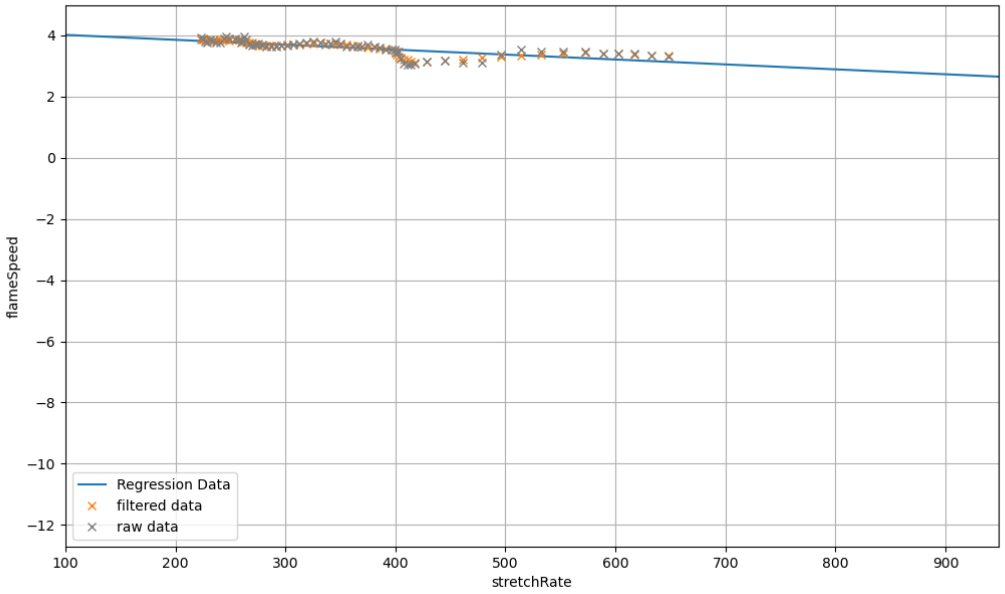

Figure D.2. Regression data, filtered data, and raw data to determine the flame speed with respect to stretch rate from Test 36

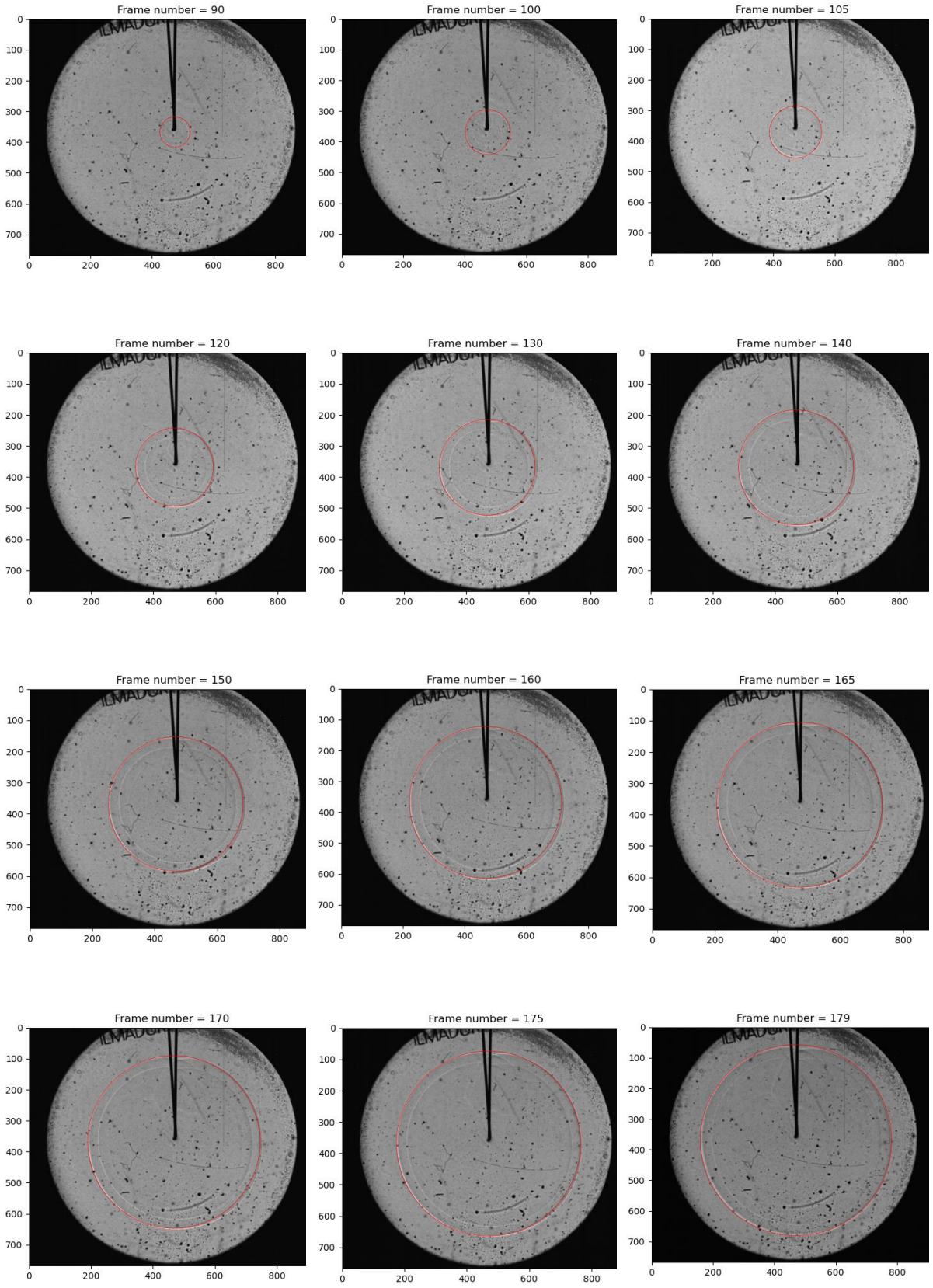

Figure D.3. Illustration on flame propagations at different frame numbers from Test 36

Appendix E: Experimental results from the test number (T37) where ignition was observed.

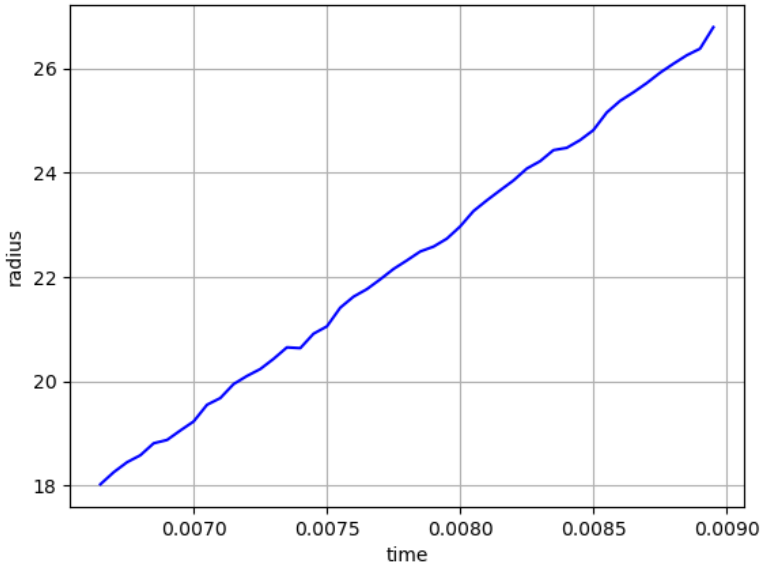

Figure E.1. Propagating flame radius with respect to time from Test 37

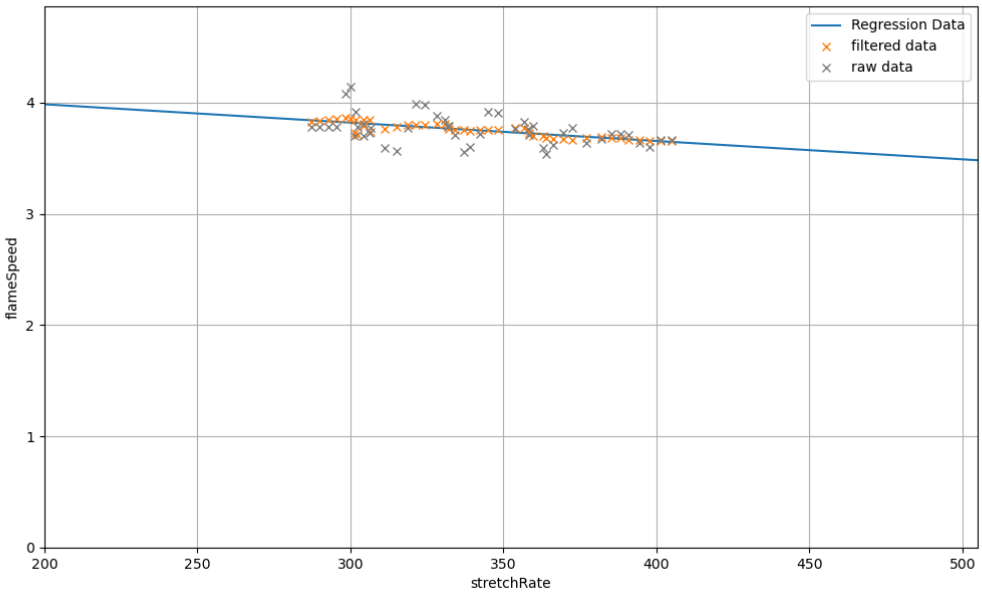

Figure E.2. Regression data, filtered data, and raw data to determine the flame speed with respect to stretch rate from Test 37

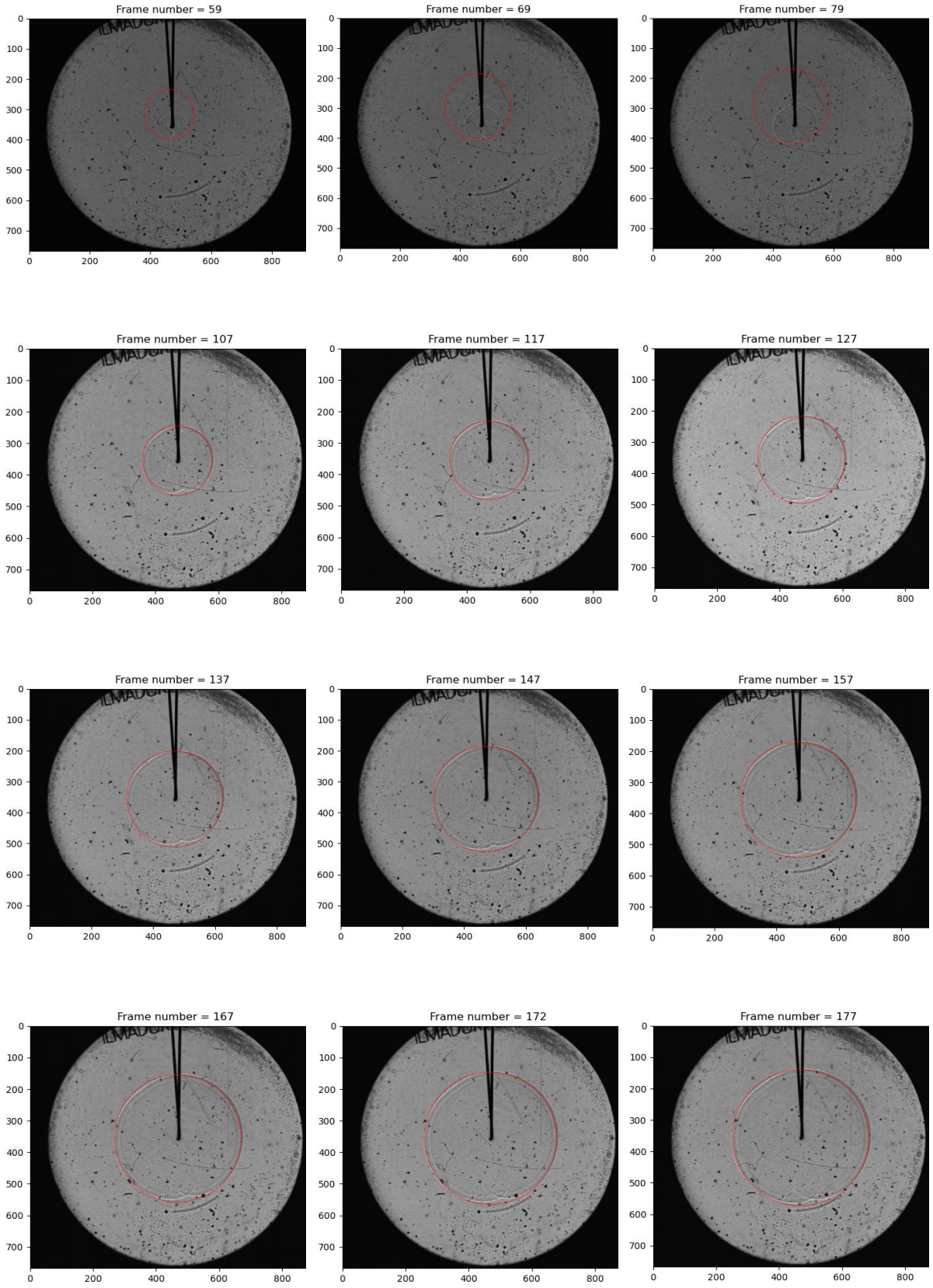

Figure E.3. Illustration on flame propagations at different frame numbers from Test 37

Appendix F: Experimental results from the test number (T39) where ignition was observed.

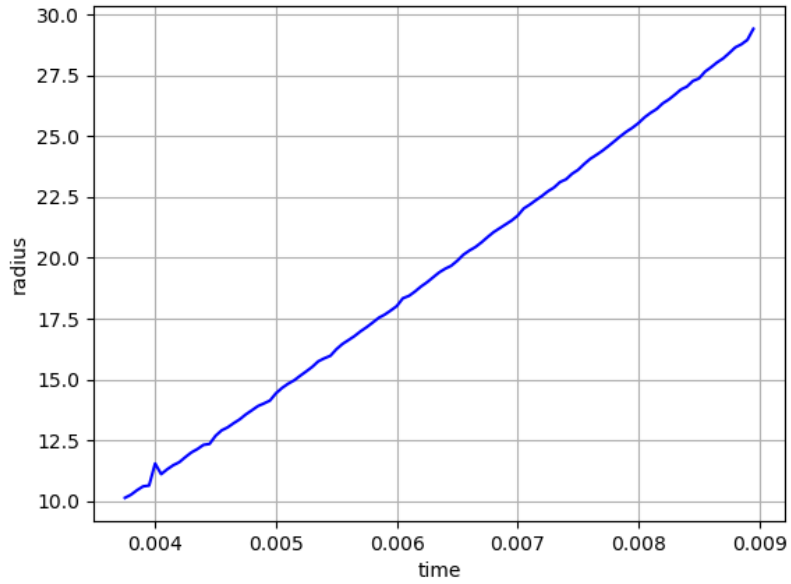

Figure F.1. Propagating flame radius with respect to time from Test 39

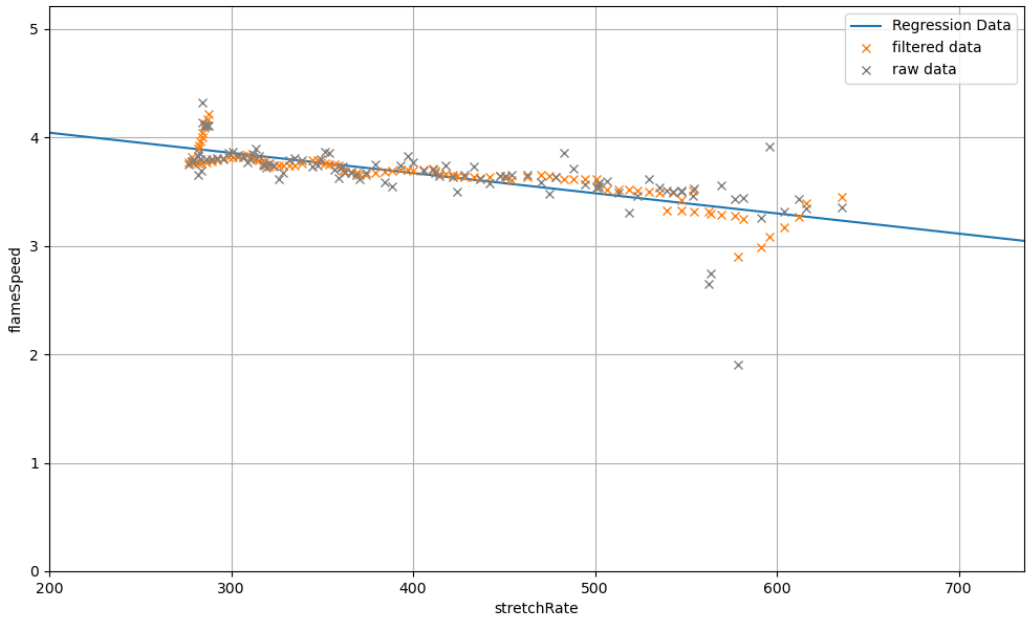

Figure F.2. Regression data, filtered data, and raw data to determine the flame speed with respect to stretch rate from Test 39

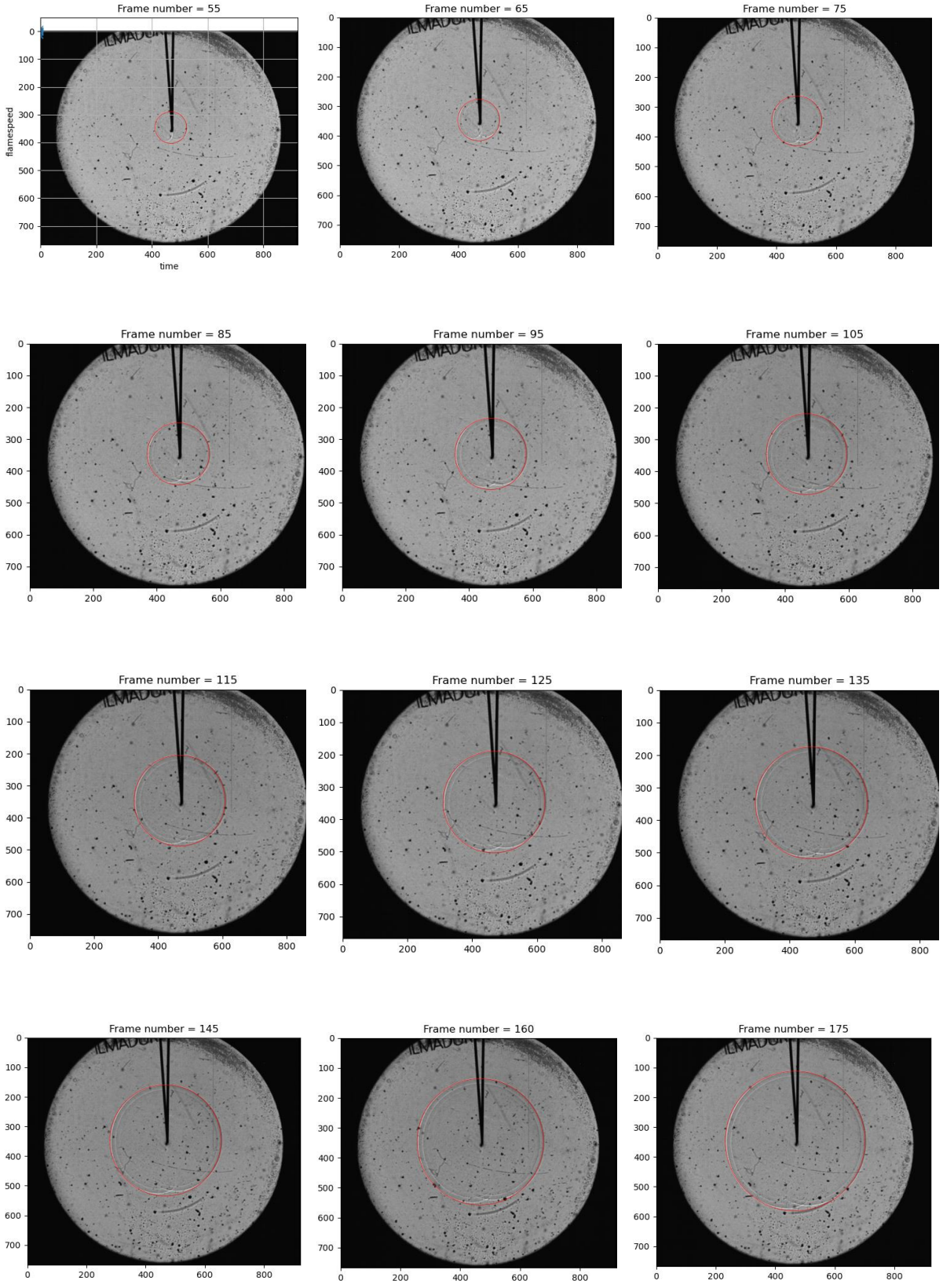

Figure F.3. Illustration on flame propagations at different frame numbers from Test 39

Appendix G: Experimental results from the test number (T47) where ignition was observed.

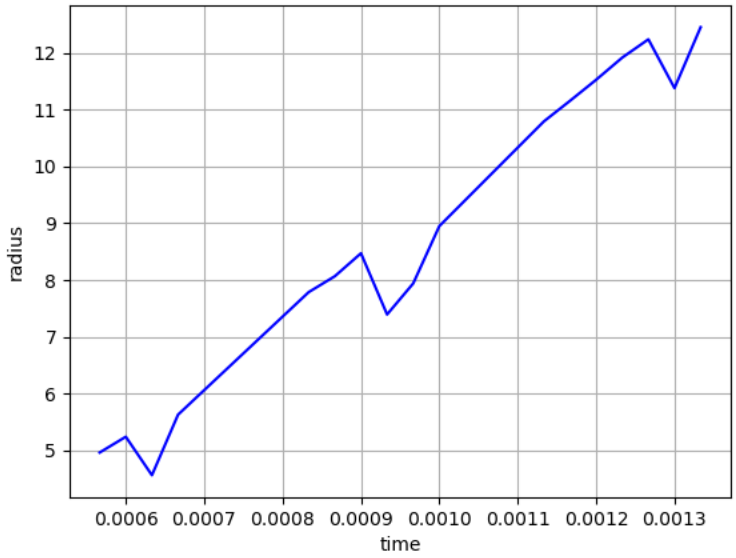

Figure G.1. Propagating flame radius with respect to time from Test 47

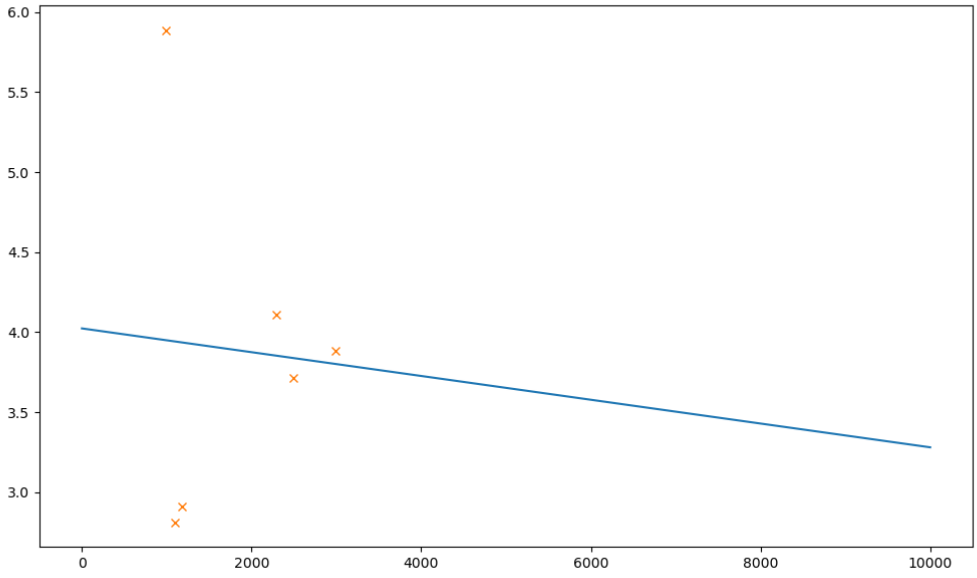

Figure G.2. Regression data, filtered data, and raw data to determine the flame speed with respect to stretch rate from Test 47

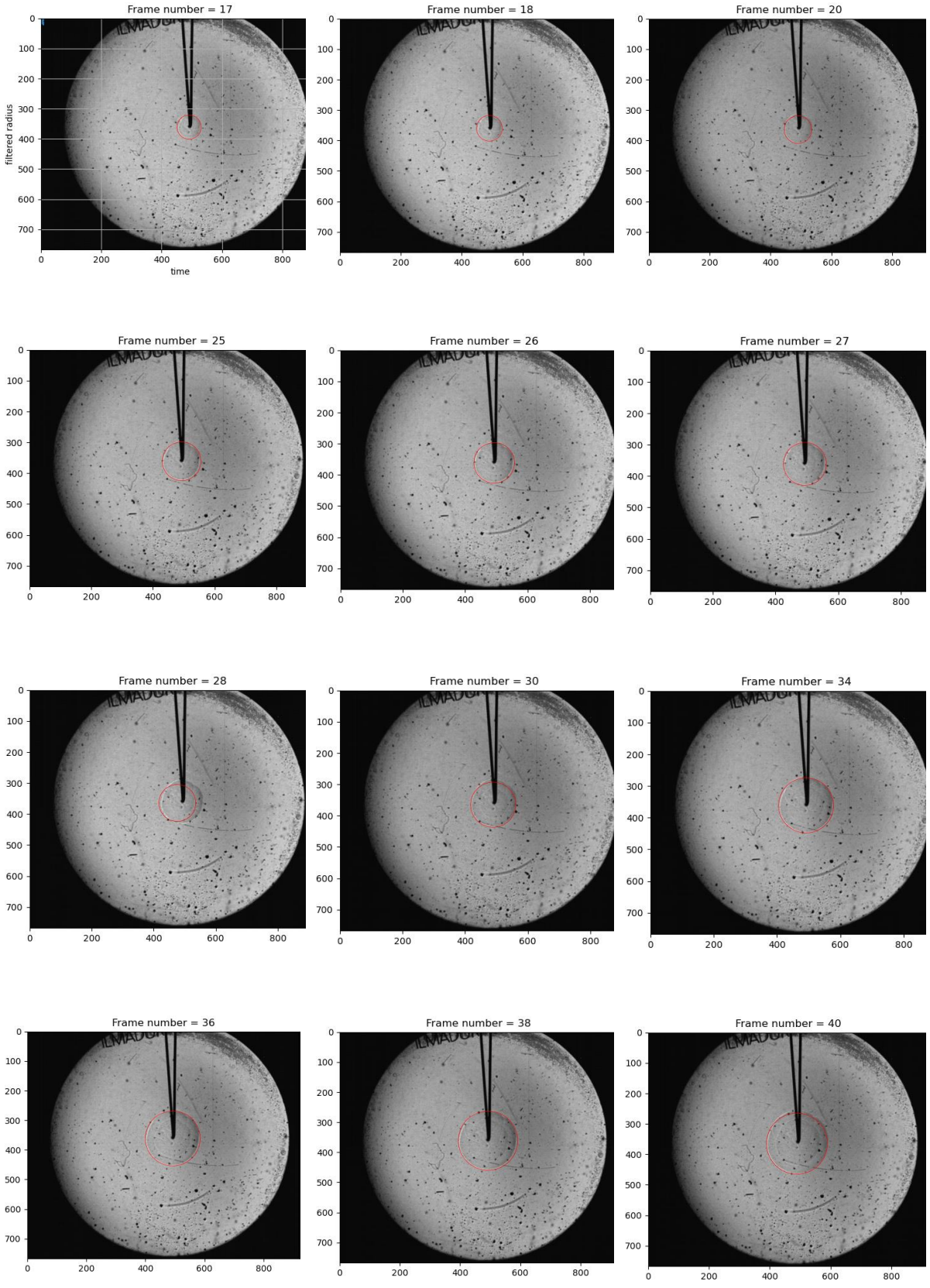

Figure G.3. Illustration on flame propagations at different frame numbers from Test 47

Appendix H: Experimental results from the test number (T48) where ignition was observed.

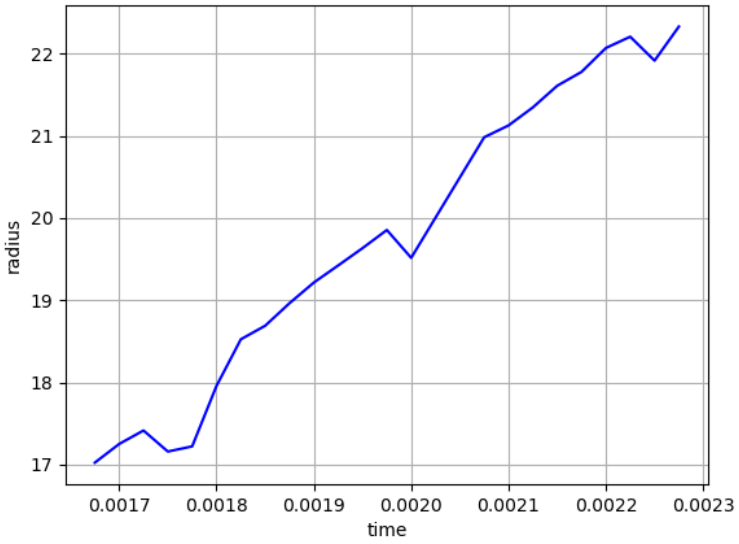

Figure H.1. Propagating flame radius with respect to time from Test 48

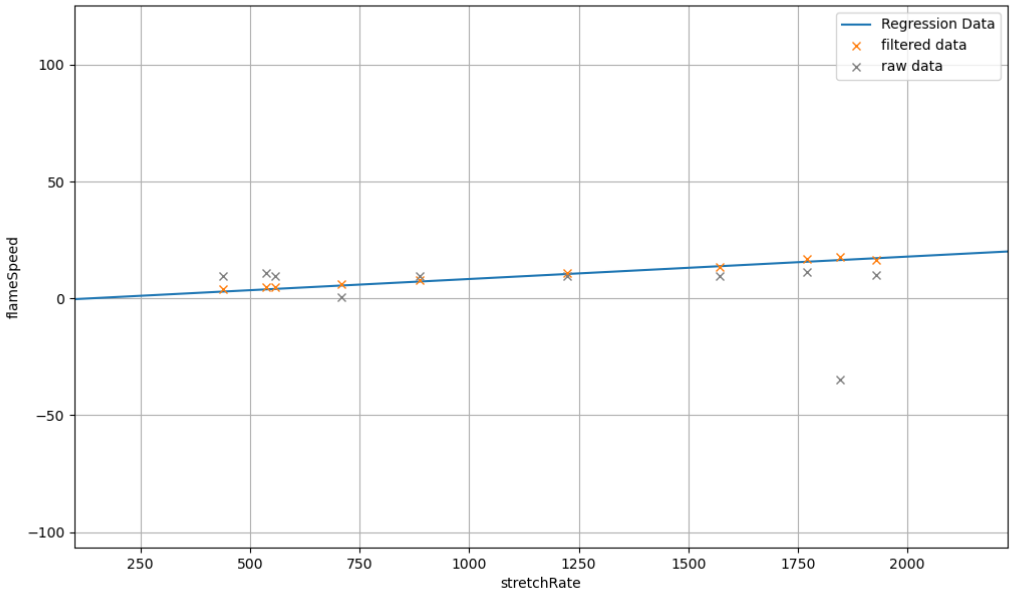

Figure H.2. Regression data, filtered data, and raw data to determine the flame speed with respect to stretch rate from Test 48

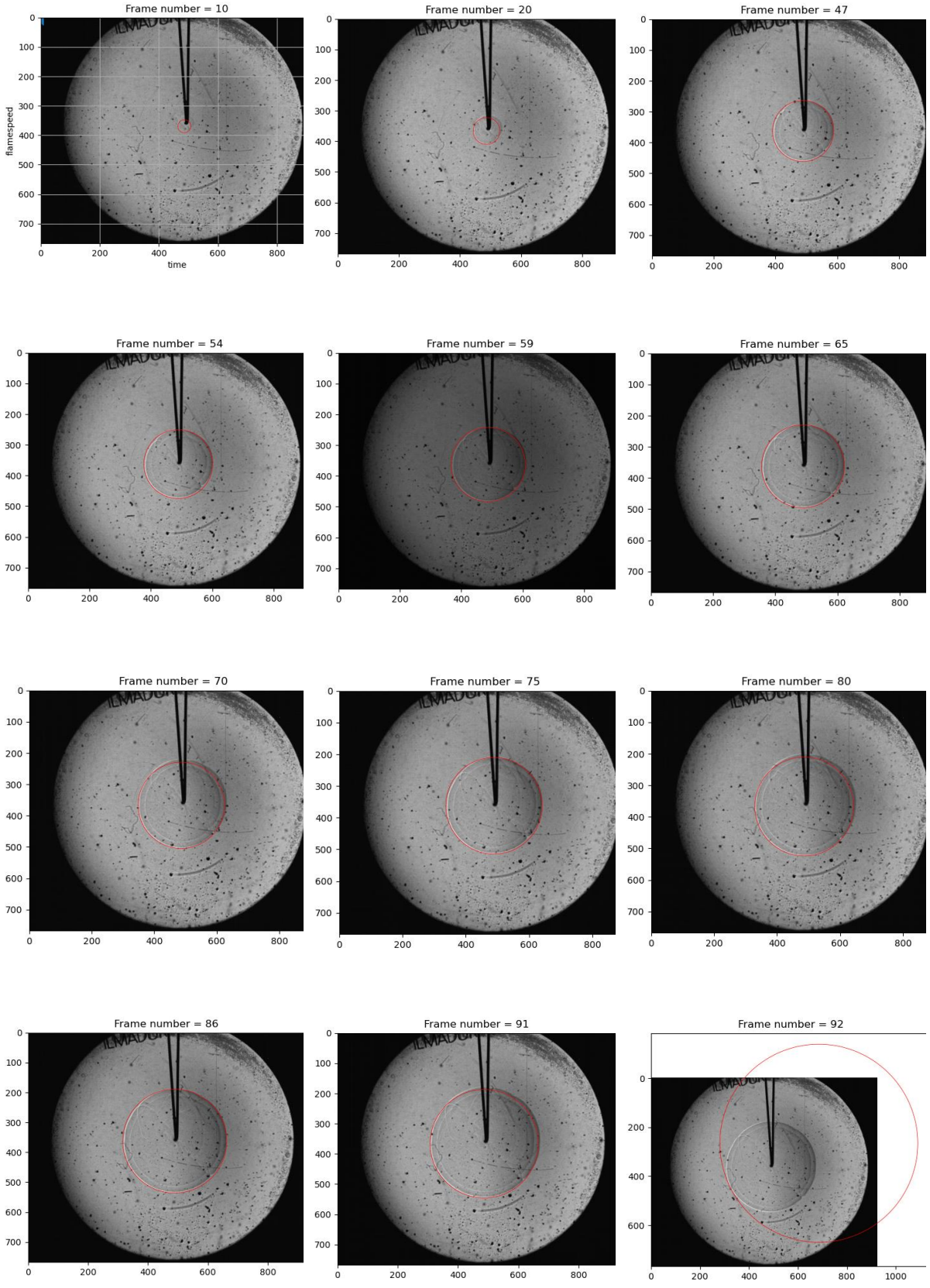

Figure H.3. Illustration on flame propagations at different frame numbers from Test 48

Appendix I: Experimental results from the test number (T57) where ignition was observed.

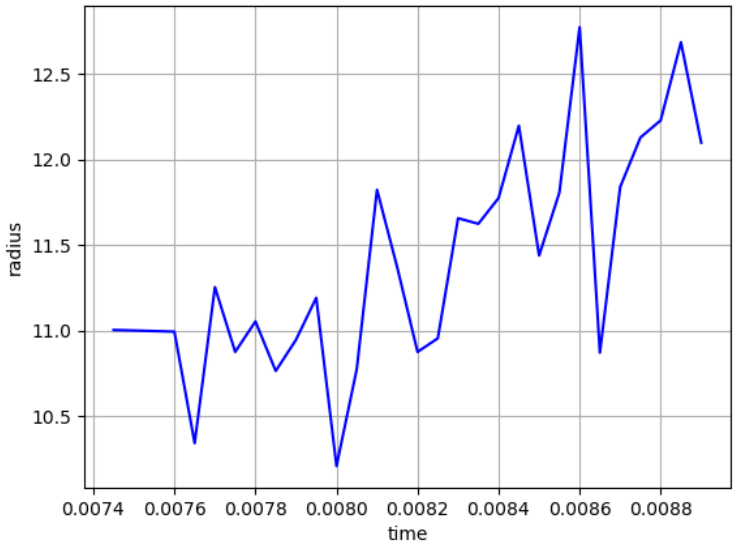

Figure I.1. Propagating flame radius with respect to time from Test 57

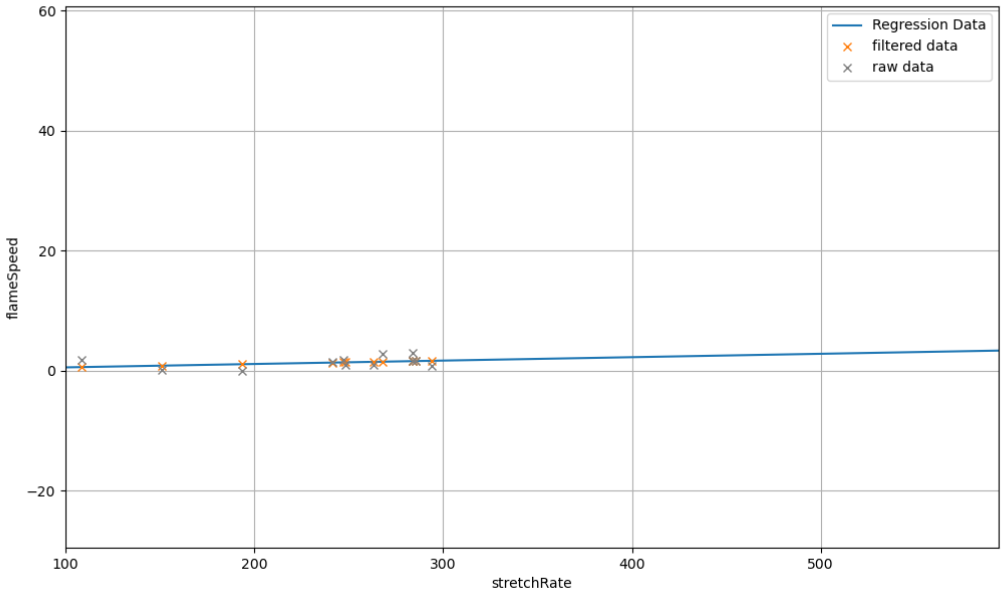

Figure I.2. Regression data, filtered data, and raw data to determine the flame speed with respect to stretch rate from Test 57

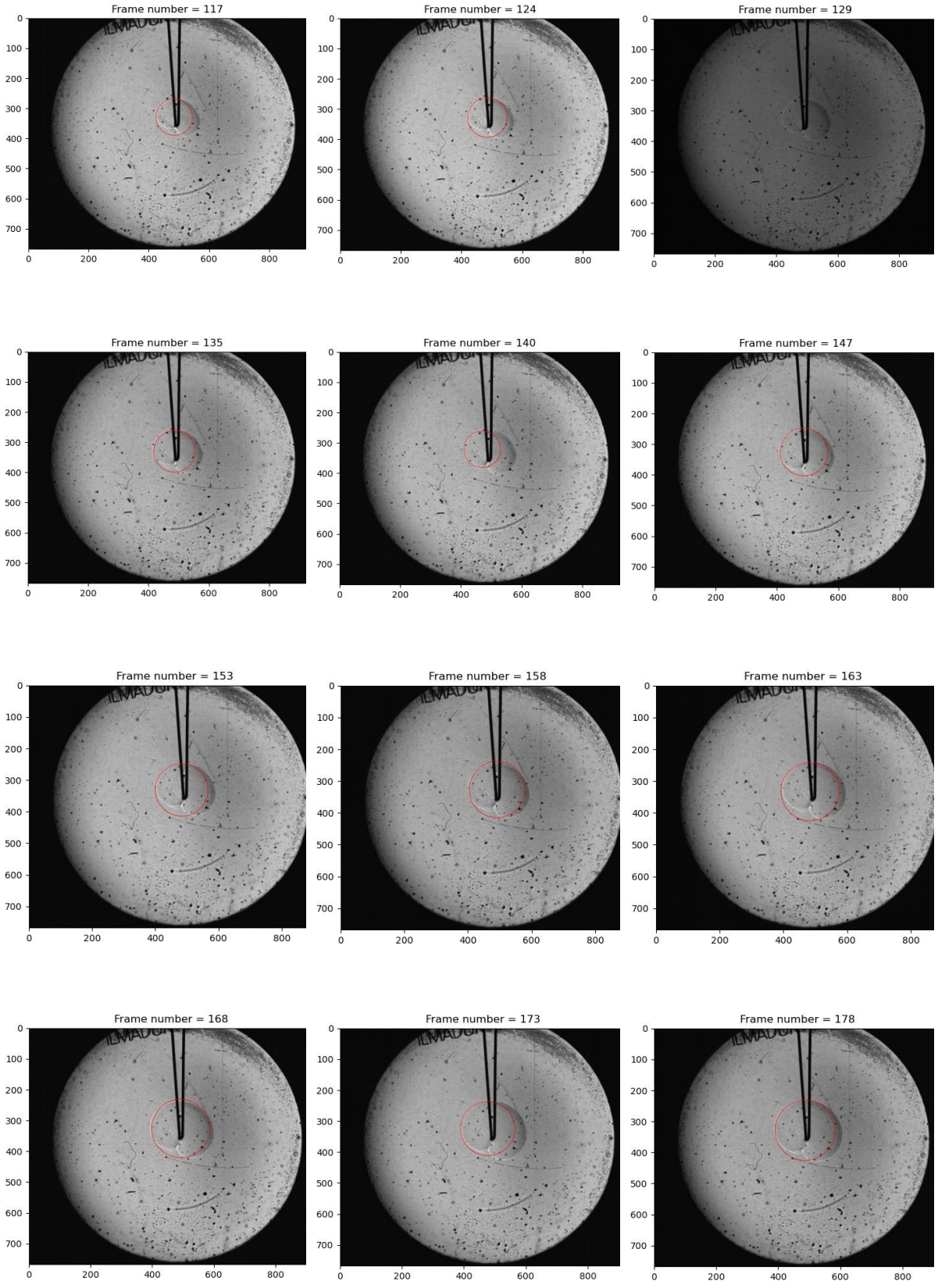

Figure I.3. Illustration on flame propagations at different frame numbers from Test 57

Appendix J: Experimental results from the test number (T69) where ignition was observed.

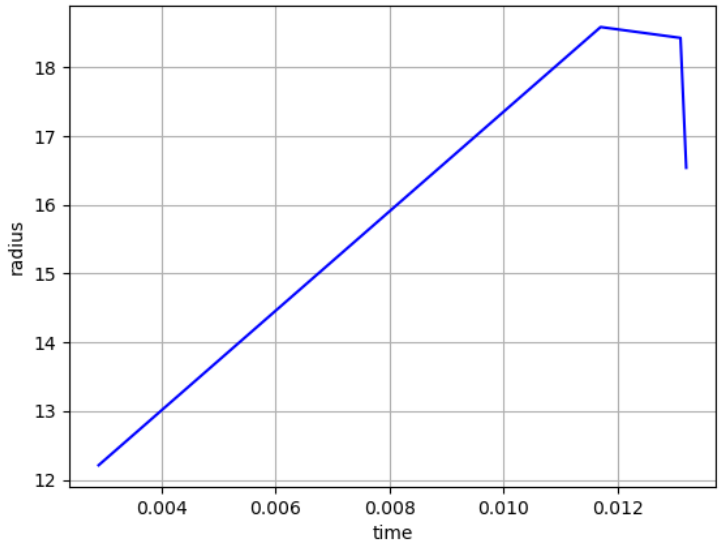

Figure J.1. Propagating flame radius with respect to time from Test 69

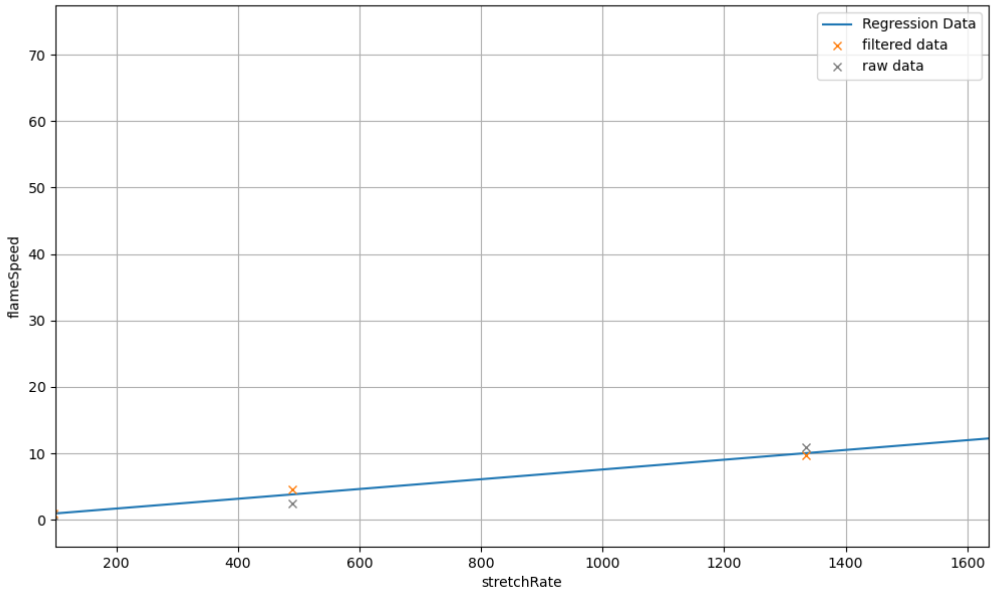

Figure J.2. Regression data, filtered data, and raw data to determine the flame speed with respect to stretch rate from Test 69

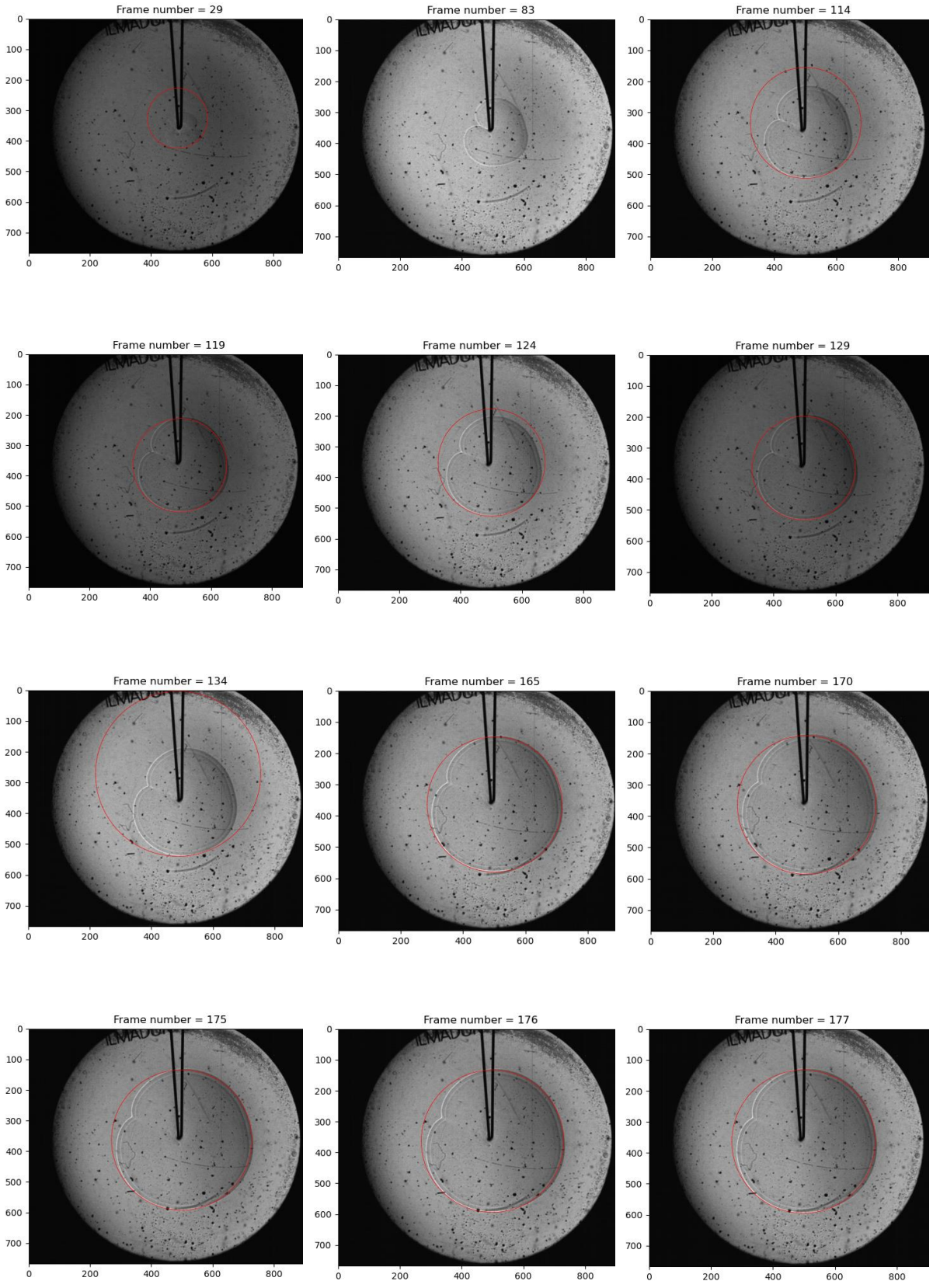

Figure J.3. Illustration on flame propagations at different frame numbers from Test 69

Appendix K: Experimental results from the test number (T71) where ignition was observed.

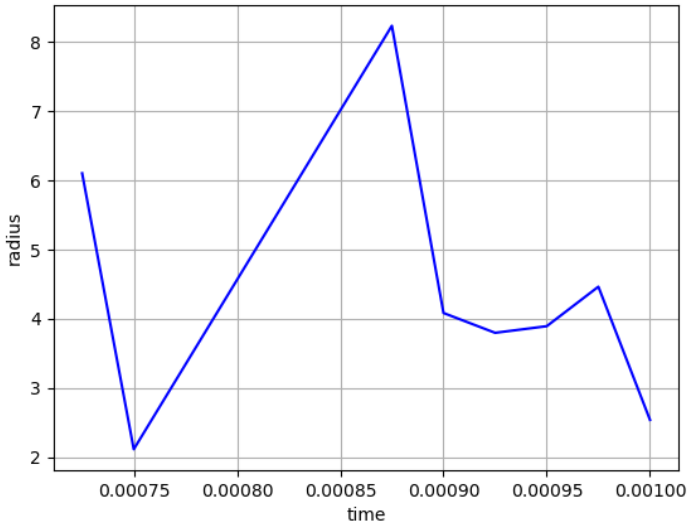

Figure K.1. Propagating flame radius with respect to time from Test 71

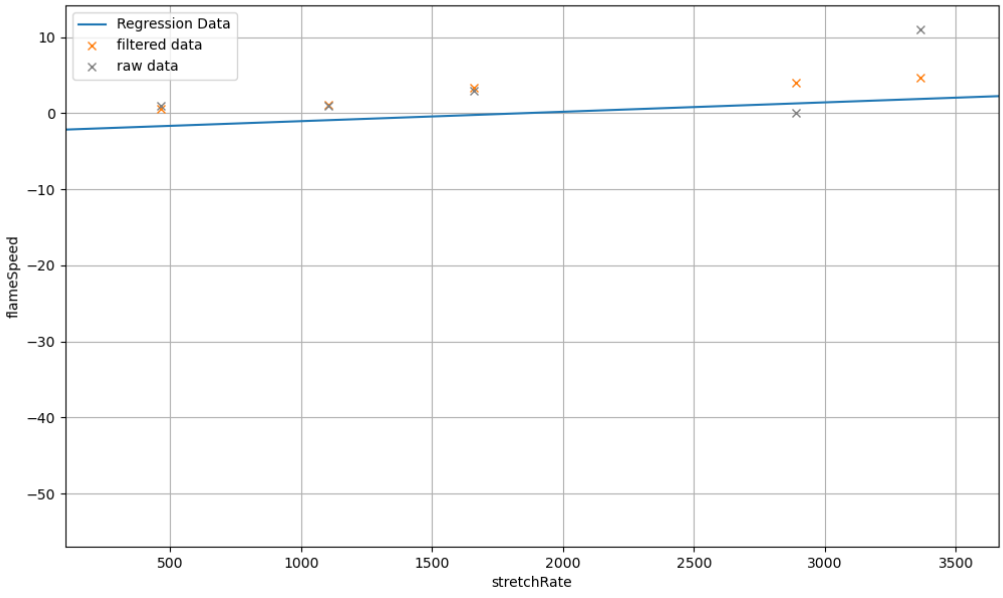

Figure K.2. Regression data, filtered data, and raw data to determine the flame speed with respect to stretch rate from Test 71

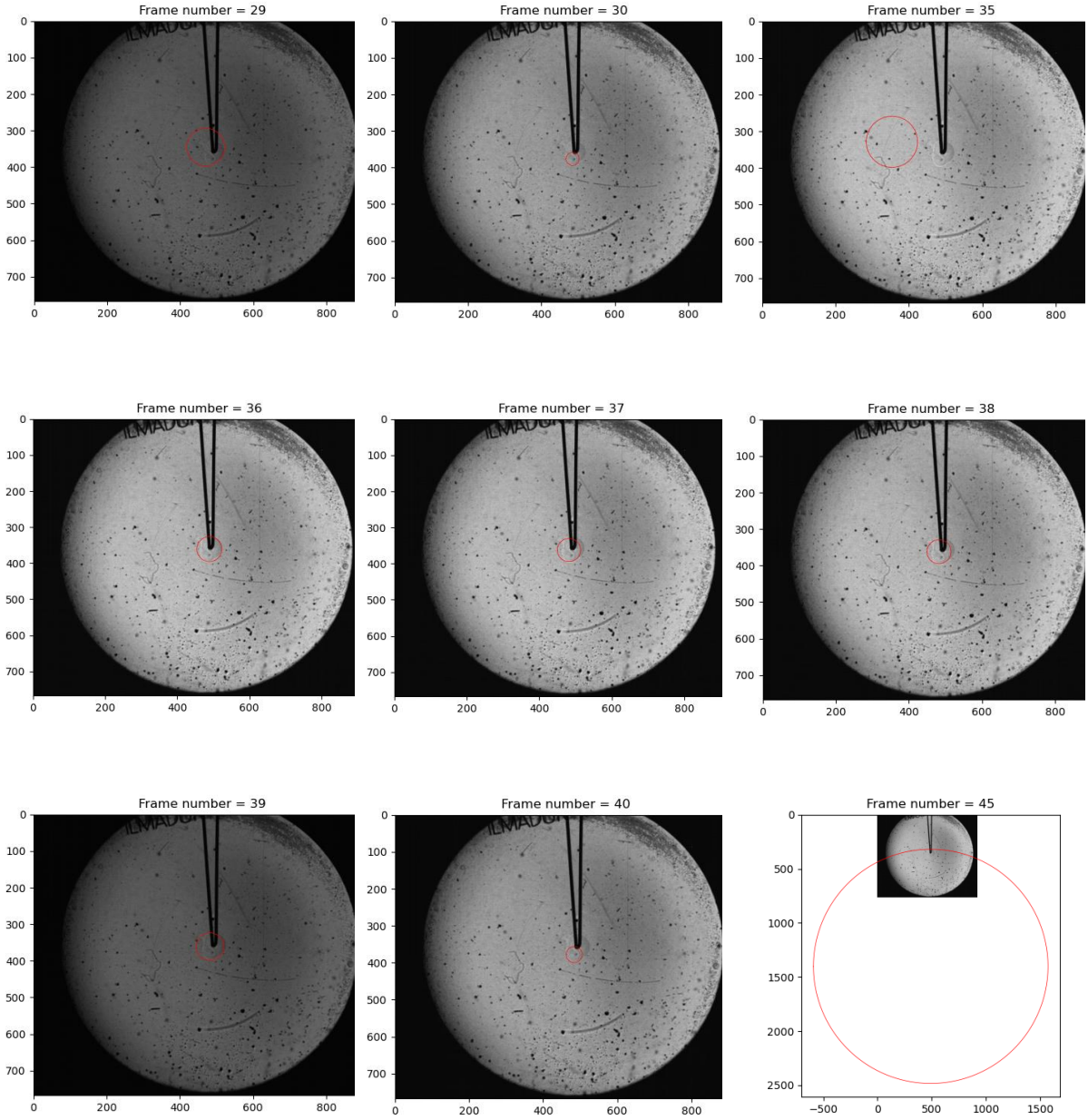

Figure K.3. Illustration on flame propagations at different frame numbers from Test 71

Appendix L: The initial conditions and input data used for the experimental tests

Table L.1. Input data from the experimental tests

Test Number	Type of fuel	Concentration target	Set vessel temp	Initial Pressure	Partial pressure with fuel after filling	Partial pressure with N2	Partial pressure with Air
12	H2/O2/N2	29.58%,14.79%,55.63%	27	100.7	395.6	0	606.9
13	H2/O2/N2	29.58%,11.83%,58.59%	27	100.7	395.5	140.3	466
14	H2/O2/N2	29.58%,8.87%,61.55%	27	101.2	396.3	280.3	325.2
36	H2/O2/N2	29.58%,7.39%,63.03%	27	101.3	396.8	352.6	256
37	H2/O2/N2	29.58%,7.39%,63.03%	27	100.9	395.4	351.5	253
39	H2/O2/N2	29.58%,7.39%,63.03%	27	101.6	398.2	351.3	250.5
47	H2/O2/N2	25.15%,15.72%,59.13%	27	100.7	352.6	0	645.5
48	H2/O2/N2	25.15%,12.57%,62.28%	27	100.8	357.7	149.9	492.2
57	H2/O2/N2	25.15%,6.29%,68.56%	27	100.6	352	449.3	199.8
69	H2/O2/N2	25.15%,6.29%,68.56%	27	100	351.4	452.7	193.6
71	H2/O2/N2	25.15%,7.86%,66.99%	27	101.2	353.5	374.7	268

Table L.2. Input data from the experimental tests (Continuation of Table L.1)

Test Number	Type of fuel	Concentration target	lambda	Total Pressure	Capacitor pF	Volatge Power Supply	Charge time
12	H2/O2/N2	29.58%,14.79%,55.63%	1	1002	10	5	50
13	H2/O2/N2	29.58%,11.83%,58.59%	0.8	999.4	10	5	50
14	H2/O2/N2	29.58%,8.87%,61.55%	0.6	1001.5	10	5	50
36	H2/O2/N2	29.58%,7.39%,63.03%	0.5	1005.4	20,000	5	1000
37	H2/O2/N2	29.58%,7.39%,63.03%	0.5	999.9	10,000	5	1000
39	H2/O2/N2	29.58%,7.39%,63.03%	0.5	1000	5000	5	500
47	H2/O2/N2	25.15%,15.72%,59.13%	1	998.1	100	5	50
48	H2/O2/N2	25.15%,12.57%,62.28%	0.8	999.8	100	5	50
57	H2/O2/N2	25.15%,6.29%,68.56%	0.4	1001.1	20,000	5	1000
69	H2/O2/N2	25.15%,6.29%,68.56%	0.4	997.7	30,000	5	2000
71	H2/O2/N2	25.15%,7.86%,66.99%	0.5	996.2	100	5	50

Table L.3. Input data from the experimental tests (Continuation of Table L.1)

Test Number	Type of fuel	Concentration target	End temp	FPS	Ignition (Yes/No)
12	H2/O2/N2	29.58%,14.79%,55.63%	27	20,000	Yes
13	H2/O2/N2	29.58%,11.83%,58.59%	27.1	50,000	Yes
14	H2/O2/N2	29.58%,8.87%,61.55%	27.2	30,000	Yes
36	H2/O2/N2	29.58%,7.39%,63.03%	26.9	10,000	Yes*
37	H2/O2/N2	29.58%,7.39%,63.03%	26.8	20,000	Yes
39	H2/O2/N2	29.58%,7.39%,63.03%	26.9	20,000	Yes
47	H2/O2/N2	25.15%,15.72%,59.13%	26.8	30,000	Yes
48	H2/O2/N2	25.15%,12.57%,62.28%	26.9	40,000	Yes
57	H2/O2/N2	25.15%,6.29%,68.56%	26.9	20,000	Yes
69	H2/O2/N2	25.15%,6.29%,68.56%	27.1	10,000	Yes
71	H2/O2/N2	25.15%,7.86%,66.99%	27.2	40,000	Yes

Appendix M: The output data obtained from the experimental tests

Table M.1. Output data from the experimental tests

Test Number	Partial Pressure H2 [mbar]	Partial Pressure O2 [mbar]	Partial Pressure N2 [mbar]	Total Pressure [mbar]	lambda [-]	Fuel-Air Equilibrium [-]	Fuel-Oxygen Equilibrium [-]
12	294.9	148.6	559.004	1002	1.00	0.99	0.99
13	294.8	119.0	587.993	999.4	0.80	0.99	1.24
14	295.1	89.5	617.156	1001.5	0.60	0.99	1.65
36	295.5	75.0	634.867	1005.4	0.50	0.99	1.97
37	294.5	74.3	631.081	999.9	0.50	0.99	1.98
39	296.6	73.9	629.459	1000	0.50	1.00	2.01
47	251.9	156.7	589.498	998.1	1.00	0.80	0.80
48	256.9	124.5	618.37	999.8	0.80	0.82	1.03
57	251.4	63.1	686.616	1001.1	0.40	0.80	1.99
69	251.4	61.7	684.644	997.7	0.39	0.80	2.04
71	252.3	77.5	666.368	996.2	0.50	0.81	1.63

Table M.2. Output data from the experimental tests (Continuation of Table M.1)

Test Number	Laminar Burning Velocity [m/s]	Laminar Flame Speed [m/s]	Markstein length [m]	Sigma	Adiabatic [K]	Cantera Laminar Burning Velocity [m/s]	Cantera Laminar Flame Speed [m/s]
12	2.17	14.71	0.0002	6.79	2367.1	2.35	15.94
13	1.95	11.92	0.0007	6.12	2085.3	2.08	12.76
14	1.33	6.78	0.0003	5.09	1677.9	1.42	7.23
36	0.92	4.17	0.0016	4.52	1469.5	0.88	3.98
37	0.95	4.31	0.0016	4.52	1469.5	0.88	3.98
39	0.98	4.41	0.0019	4.52	1469.5	0.88	3.98
47	0.64	4.02	0.0001	6.28	2154.1	1.66	10.43
48	0.21	1.29	(-)0.0095	6.12	2116.5	2.08	12.76
57	0.01	0.04	(-)0.0057	4.08	1310.5	0.42	1.7
69	0.05	0.22	0.0074	4.08	1310.5	0.42	1.7
71	0.48	2.27	(-)0.0012	4.7	1534.7	0.93	4.37